Discovery of broad-spectrum bacterial polyamine detoxification inhibitors as potential antivirulence agents and antibiotic adjuvants

Peri B. Moulding[1], Ronald S. Flannagan[2], Jonas Wong[3,4,5,6,7], Ahmed M. Soliman[1,8], Wael Elhenawy[3,4,5,6,7], David E. Heinrichs[2], and Omar M. El-Halfawy[1,9*]

[1] Department of Chemistry and Biochemistry, Faculty of Science, University of Regina, Regina, SK, S4S 0A2, Canada

[2] Department of Microbiology and Immunology, University of Western Ontario, London, Ontario, Canada

[3] Department of Medical Microbiology & Immunology, Faculty of Medicine & Dentistry, University of Alberta, Canada.

[4] Li Ka Shing Institute of Virology, Canada.

[5] Women and Children's Health Research Institute, Edmonton, Alberta, Canada.

[6] Antimicrobial Resistance, One Health Consortium - Edmonton, AB, Canada.

[7] Striving for Pandemic Preparedness - The Alberta Research Consortium - Edmonton, AB, Canada.

[8] Department of Microbiology and Immunology, Faculty of Pharmacy, Kafrelsheikh University, Kafr El-Sheikh 33516, Egypt

[9] Department of Microbiology and Immunology, Faculty of Pharmacy, Alexandria University, Alexandria, 21521, Egypt

[*] Correspondence: omar.el-halfawy@uregina.ca (O.M.E.)

Running title: Broad-spectrum polyamine detoxification inhibitors

Abstract

Bacteria continue to develop resistance against antibiotics, including last-resort ones, reinforcing the urgent need for new antimicrobial strategies. Chemicals at infection sites in the host often influence microbial virulence and antibiotic response; such interactions may offer new antimicrobial targets. Polyamines are cationic small molecules bacteria may encounter at infection sites. They are overproduced during infection, modulating host immune responses. The ability of bacteria to detoxify polyamines such as by a spermine/spermidine acetyltransferase (SpeG) correlated with hypervirulence of pathogens, including *Salmonella* Typhimurium, *Enterococcus faecium*, and the community-acquired methicillin-resistant *Staphylococcus aureus* (MRSA) strain USA300. Polyamines may also influence bacterial antibiotic response. For example, we found that USA300 uses exogenous polyamines to resist antibiotics, including vancomycin, a phenotype lost in the Δ*speG* mutant. Therefore, we aimed to uncover inhibitors of polyamine detoxification. A high-throughput chemical screen against *S. aureus* USA300 identified OES2-0017, which showed potent synergy with polyamines and growth-inhibitory effects at the low micromolar range. We revealed a dual mode of action of OES2-0017, where low concentrations inhibited SpeG and other polyamine detoxification enzymes, and higher concentrations perturbed the bacterial membrane. Eukaryotic cell membranes were not impacted at the same concentration range, as observed in a hemolysis assay. OES2-0017 abolished the polyamine-mediated antibiotic resistance in MRSA USA300, suggesting its potential utility as an antibiotic adjuvant. Notably, OES2-0017 showed similar polyamine synergy and growth inhibitory activities against other Gram-positive (e.g., *E. faecium* and *E. faecalis*) and Gram-negative (e.g., *Klebsiella pneumoniae*, *S.* Typhimurium, and *Burkholderia cenocepacia*) pathogens. OES2-0017 prevented *S.* Typhimurium from replicating in murine macrophages, which also suggests its potential application as an antivirulence agent. Together, this work exploits understudied aspects of chemically mediated host-pathogen interactions, offering a potential new antimicrobial strategy with a novel mode of action for multidrug-resistant priority pathogens.

Introduction

Bacteria have developed resistance to all currently available antibiotics posing a large public health risk. The spread of antimicrobial resistance (AMR) has exacerbated the threat of bacterial infections, with 1.27 million deaths directly attributed to bacterial AMR in 2019 alone (*1*). *Staphylococcus aureus* is a leading cause of hospital and community-acquired infections, resulting in considerable morbidity and mortality rates (*2*). *S. aureus* can cause multiple infections, including skin and soft tissue infections (SSTI), infective endocarditis, osteomyelitis, prosthetic-device infections, community-acquired pneumonia, and other systemic infections (*3*). Some strains of *S. aureus* have developed resistance to β-lactam antibiotics, coined methicillin-resistant *Staphylococcus aureus* (MRSA). MRSA strains have spread rapidly, and in 2019 alone, it was estimated that more than 100,000 deaths were directly attributable to MRSA infections worldwide (*1*). Notably, the MRSA strain USA300 has become the most common infection-causing *S. aureus* strain in Canada and the USA (*4, 5*).

While we continue to lose clinically useful antibiotics due to the rise of AMR, the discovery and development of antimicrobials with novel chemical structures or cellular targets has drastically slowed (*6, 7*). One of the potential reasons for the antibiotic discovery void is that antimicrobial discovery efforts traditionally relied on antimicrobial susceptibility testing (AST) conditions that use culture media such as Mueller-Hinton broth (MHB) (*8*). These test conditions do not accurately reflect those at the infection site, including the chemicals bacteria may encounter within the host. There is an expansive array of molecules produced by the host, resident microbiota, and the infecting pathogen at the infection site, which may influence microbial virulence and antibiotic responses (*9, 10*). Such chemical-mediated effects might alter the treatment outcomes and may offer new targets for antimicrobial intervention. One prominent class of compounds is polyamines, which are biogenic small cationic amines, such as the diamine putrescine, triamine spermidine, and tetramine spermine, required for normal cell functioning in most living organisms (*11*). Polyamines are overproduced by the host in response to infection (*12-14*), and can be found at millimolar concentrations in eukaryotes (*15, 16*), where they have immunomodulatory roles (*17, 18*).

Most bacteria produce polyamines endogenously, with *S. aureus* being one of few exceptions that neither produce spermine or spermidine nor require them for homeostasis (*19-21*). For polyamine producers, polyamine levels are tightly regulated to maintain the

level required for homeostasis, balancing uptake and biosynthesis with detoxification and efflux to prevent toxicity resulting from high and low polyamine cellular content (*11, 16*). On the contrary, most *S. aureus* strains, being polyamine non-producers, are typically more susceptible to these compounds; however, USA300 is resistant to exogenous spermine and spermidine (*19*). The virulence and prevalence of USA300 have been partially attributed to the acquisition of the arginine catabolic mobile element (ACME) (*14, 22, 23*). The ACME was horizontally transferred to *S. aureus* from *Staphylococcus epidermidis*, and encodes SpeG, a member of the GCN5-related *N*-acetyltransferase (GNAT) family (*23*). SpeG is a spermine/spermidine *N*-acetyltransferase (SSAT) that acetylates spermine and spermidine rendering them less toxic to the cell, resulting in the observed resistance to exogenous polyamines (*14, 19, 20, 23*). The ACME also encodes the arginine-deaminase (*arc*) system which converts arginine to ornithine while producing ATP and ammonia, allowing USA300 to withstand acidic environments, such as those found on the skin (*14*). The host then converts ornithine produced via the ACME-Arc system to polyamines as shown in a murine SSTI model (*14*). Therefore, by carrying *speG,* USA300 can resist the excessive host polyamine production, increasing its virulence. Additionally, exogenous polyamines increase biofilm formation, an effect lost in a Δ*speG* mutant (*23*).

Polyamine detoxification via SSAT homologs contributed to virulence in other bacterial species. For example, SpeG is required for the survival of *Salmonella enterica* serovar Typhimurium in macrophages (*24*) and the overexpression of PmvE in *Enterococcus faecalis* increases virulence in a *Galleria mellonella* infection model (*25*). Polyamines are also known to alter bacterial susceptibility to antibiotics (*26-30*) and to influence virulence phenotypes such as biofilm formation (*31-33*), intracellular growth (*34*), colonization (*35*), and resistance to reactive oxygen species (*36*). Given the correlation of the ability of pathogens to detoxify polyamines with their hypervirulence and the potential for polyamine-mediated alterations to antibiotic susceptibility at the site of infection, inhibiting bacterial polyamine detoxification appears as an attractive strategy to reduce virulence and prevent polyamine-mediated antibiotic resistance. Indeed, new treatment strategies to combat the spread of AMR are desperately needed, and antivirulence agents and antibiotic adjuvants have been suggested as potential therapeutic options. Antivirulence agents target processes dispensable for bacterial viability but that the pathogen uses to cause infection; therefore, by targeting these processes the host immune system can more easily clear the infection (*37*). Antibiotic adjuvants are compounds that potentiate the activity of existing

122 antibiotics, restoring their effect against resistant bacteria or improving their efficacy against
123 intrinsically resistant organisms (*38*).
124 Here, we set out to identify inhibitors of bacterial polyamine detoxification
125 mechanisms through a cell-based high throughput screen against *S. aureus* USA300, as it
126 lacks *de novo* polyamine biosynthesis. We discovered the polyamine analog OES2-0017,
127 which showed potent synergy with polyamines (a phenotype lost in SSAT mutants) and
128 growth-inhibitory effects at the low micromolar range against various Gram-positive and
129 Gram-negative pathogens. We revealed a dual mode of action of OES2-0017, where low
130 concentrations inhibited SpeG and other polyamine detoxification enzymes, and higher
131 concentrations perturbed the bacterial membrane in *S. aureus*. Eukaryotic cell membranes
132 were not impacted at the same concentration range, as observed in a hemolysis assay. The
133 inhibitor eradicated SpeG-expressing *S.* Typhimurium inside murine macrophages,
134 suggesting its potential as an antivirulence agent. OES2-0017, at the low polyamine-
135 synergistic concentrations, abolished the polyamine-mediated resistance of MRSA USA300
136 to vancomycin and other antibiotics, suggesting its potential utility as an antibiotic adjuvant.
137 We also uncovered previously uncharacterized alternative polyamine detoxification
138 mechanisms in *S. aureus* that OES2-0017 inhibited. Our screen also uncovered additional
139 inhibitors, including the catechol derivative, isoproterenol, OES1-1087, showing similar
140 mode of action and activity as OES2-0017 but with lower potency. Together, this study
141 describes novel antimicrobial compounds with broad-spectrum activity and potential
142 antivirulence and antibiotic adjuvant applications.
143

144 **Materials and methods**
145 **Bacterial strains and reagents.** Table S1 and S2 list strains, plasmids and primers
146 used in this work. Bacteria were grown in Mueller Hinton medium at 37°C. Except for
147 *Enterococcus faecalis* and *Enterococcus faecium*, which were grown in Tryptic Soy Broth
148 and *Mycobacterium smegmatis,* which was grown in Luria Broth.
149 **Antimicrobial susceptibility testing.** Minimum inhibitory concentration (MIC) and
150 checkerboard assays were performed using the CLSI broth microdilution technique (*8*). The
151 fractional inhibitory concentration indices (FICI) were calculated as FICI=($MIC_{drug\ A}$ in
152 combination/$MIC_{drug\ A}$ alone)+($MIC_{drug\ B}$ in combination)/$MIC_{Drug\ B}$ alone). FICI values were

153 interpreted as synergy when FICI ≤ 0.5, no interaction when 1 ≤ FICI ≤ 4, and antagonism
154 when FICI > 4.0.

155 **Chemical screen and polyamine analog library assembly.** I assembled a library
156 of polyamine analogs by selecting analogs of polyamines and closely related molecules with
157 a cut-off of 60% structural similarity from a chemical supplier. This library was screened at
158 20 μM or 5 mM in the presence and absence of spermine at 1/4th the wild-type MIC. Library
159 compounds were added to 96-well plates and filled with inoculated MHB. A library of
160 previously approved drugs and natural product derivatives was screened at 20 μM against
161 the wild-type USA300 strain in the presence of spermine at 1/4th the wild-type MIC.
162 Compounds were administered to 384-well plates containing inoculated MHB with spermine
163 using the Biomatrix BM5-BC (S&P Robotics inc.). Plates were incubated at 37°C, and
164 bacterial growth was determined turbidimetrically after 24 hours.

165 ***S. aureus* Nebraska Transposon Mutant Library (NTML) screen.** Overnight
166 cultures of the NTML (*39*) were prepared in 384-well plates using Biomatrix BM5-BC (S&P
167 Robotics inc.) in MHB containing 5 μg/mL erythromycin. The following day, MHB containing
168 1/8th and 1/16th the wild-type MIC of spermine were inoculated using the Biomatrix BM5-BC.
169 Plates were grown at 37°C, and OD_{600} was read after 24 h.

170 ***B. subtilis* CRISPRi essential gene knockdown library screen.** Overnight
171 cultures of the library (*40*), were prepared in 96-well plates using Biomatrix BM5-BC (S&P
172 Robotics inc.) in MHB containing 6 μg/mL chloramphenicol. The following day, MHB
173 containing OES2-0017 at the wild-type MIC and at 2-fold dilutions to 1/16th the MIC, and in
174 the absence of OES2-0017 were inoculated using the Biomatrix BM5-BC. The experiment
175 was performed with 0.05% xylose (allowing low level of *dcas9* expression) and without
176 xylose (allowing basal *dcas9* expression). Plates were incubated at 37°C, and OD_{600} was
177 read after 24 h.

178 **General molecular techniques.** Unmarked in-frame deletion of speG was
179 performed using the temperature-sensitive allelic exchange plasmid pJB38 (*41*). Roughly 1-
180 kb upstream and downstream of *speG* were amplified through PCR and the upstream
181 fragment digested with EcoRI, and BamHI (New England Biolabs), and the downstream
182 fragment digested with EcoRI and SalI (New England Biolabs). pJB38 was digested with
183 BamHI and SalI and fragments were ligated with T4 DNA ligase. The resultant deletion
184 plasmid pJB38-*ΔspeG* was passaged through *E. coli* DH5α and *E. coli* DC10B, before

185 electroporation into *S. aureus* USA300 JE2 (*42*). Deletion of *speG* was confirmed through
186 PCR.
187 **Membrane permeabilization assay.** Fluorometric Disc3(5) membrane
188 permeabilization assays were performed as described in (*43*).
189 **Hemolysis Assay.** The hemolysis assay was performed using defibrinated sheep
190 blood (Thermo Fisher Scientific, and Cedarlane) as previously described (*44*).
191 **Cell adhesion and cytotoxicity assays.** Madin-darby canine kidney (MDCK) cells
192 were cultured in DMEM with 10%(v/v) FBS and maintained according to the instructions. To
193 perform viability and adhesions assays MDCK cells were split and seeded into Thermo
194 Scientific™ Nunc MicroWell 96-Well Optical-Bottom Plates (cat.165305) and grown
195 overnight to confluence (~$4x10^4$ per well). Adhered and confluent MDCK cells were then
196 washed 1x with sterile PBS and treated in serum-free DMEM with DMSO as a vehicle
197 control, OES2-017 at the MIC (20 μM), or OES1-01087at the MIC (1250 μM). A 2-fold
198 dilution series was performed for each compound down to 1/8 of the MIC. Treated MDCK
199 cells were incubated for 2h at 37℃ in a 5% CO_2 incubator. Before staining, and as positive
200 control to induce disruption of the MDCK monolayer individual wells that were previously left
201 untreated were incubated with triton x-100 for 5 mins. Wells containing MDCK cells were
202 washed 1x with PBS and then incubated with TMR-wheat germ agglutin (2 μg/mL) for 10
203 min in the cold. Cells were washed twice with PBs and then fixed with 4% (v/v) PFA. To
204 measure cell viability after 2h incubation with the compounds the cells were washed 1x with
205 PBS and stained with Zombie Violet™ (Biolegend) according to the manufacturer's
206 instructions. The dye was used at a 1:500 dilution for 15 mins and after staining the cells
207 were washed twice with PBS and fixed as above. As a positive control, prior zombie violet
208 staining individual MDCK-containing wells were treated with 100% ice-cold methanol for 3
209 mins prior to zombie violet staining. Fluorescence intensities for TMR-WGA and Zombie
210 Violet™ were measured using a Biotek Synergy H4 multimode plate reader.
211
212 **Identification of homologous acetyltransferases.** *B. subtilis* BltD and PaiA protein
213 sequences were used as a query in a Position-Specific Iterative Basic Local Alignment
214 Search Tool (PSI-BLAST) search with results limited to records of *S. aureus* subsp. aureus
215 USA300_FPR3757. Results were filtered based on alignment scores (E value).

216 **Protein overexpression and purification.** *speG,* SAUSA300_2083,
217 SAUSA300_0441, and *paiA* were cloned into pET28a(+) and overexpressed under
218 conditions previously described (*20*). *SAT1* was codon optimized and synthesized from
219 cDNA and cloned into pET28a(+) (Bio Basic Canada). Lysis was achieved using a Branson
220 Sonifier 450 and the supernatant was isolated from the insoluble fraction by centrifugation
221 at 10 000 xg for 30 minutes at 4°C. His-tag batch purification was performed using His-
222 select nickel-affinity gel (Sigma-Aldrich). Purified proteins were detected on a 10%
223 acrylamide gel (Bio-Rad), by PageBlue staining solution (Fisher Scientific). Proteins were
224 quantified using the Bradford method with protein assay dye reagent concentrate (Bio-Rad),
225 following dialysis using SnakeSkin™ dialysis tubing (Fisher Scientific).
226
227 ***In vitro* SSAT enzymatic assays**
228 **Steady state kinetics.** Purified enzymes were used in spermine/spermidine *N*-
229 acetyltransferase (SSAT) colorimetric enzymatic assays as described previously (*20, 45*),
230 with modifications. Briefly, 25 µL of enzyme solution (200 ng enzyme, 100 mM Tris-HCl, pH
231 7.5, 1 mM EDTA) were added to a 96 well plate then 50 µL of freshly prepared Ellman's
232 reagent (2 mM 5, 5'-dithio-bis-(2-nitrobenzoic acid) (DTNB) (Sigma Aldrich) 100 mM Tris-
233 HCl, pH 7.5, 1 mM EDTA) was added to each well. Finally, 25 µL of substrate solution was
234 added to begin the reaction. The substrate solution consisted of a final concentration of 1
235 mM acetyl-CoA (Sigma Aldrich) with SpeG, $PaiA_{Sa}$, SAUSA300_2083, and
236 SAUSA300_0441, and 0.25 mM acetyl-CoA with SAT1 100 mM Tris-HCl, pH 7.5, 1 mM
237 EDTA with variable concentrations of polyamines. Each reaction plate contained serial
238 standards of Coenzyme A (5-150 nmol). Reactions were allowed to proceed at 37°C and
239 $A_{412\ nm}$ readings were taken each minute for 45 min. Kinetic parameters were estimated by
240 fitting with the Michaelis-Menten equation or allosteric sigmoidal equation in Graphpad
241 Prism 10.
242 **Enzymatic inhibition assays.** The colorimetric SSAT assay was performed where
243 25 µL of enzyme solution containing 200 ng enzyme, 100 mM Tris-HCl, pH 7.5, 1 mM
244 EDTA and a dilution series of inhibitor was added to a 96-well plate. The enzyme-inhibitor
245 solution was incubated at room temperature for 30 min before adding 50 µL Ellman's
246 reagent and 25 µL substrate solution to initiate the reaction. OES2-0017 and analogs in the
247 small-scale structure-activity relationship study were assayed with a substrate solution

248 including a fixed concentration of spermine ≈ K_m and 1 or 0.25 mM acetyl-CoA SpeG and
249 SAT1, respectively. OES1-1087 inhibition was assayed with a substrate solution including
250 1500 μM spermine and an AcCoA concentration ≈ K_m. Substrate solution to evaluate
251 OES2-0017 inhibition of $PaiA_{Sa}$ contained a final concentration of 1 mM acetyl-CoA and
252 spermine ≈ K_m. The reaction was monitored each minute at $A_{412\ nm}$ for 45 minutes. We
253 evaluated the decrease in absorbance when the reaction was supplemented with the
254 inhibitors compared to a positive control containing only spermine and acetyl-CoA. Data for
255 IC_{50} plots were fit to a nonlinear regression inhibition model in Graphpad Prism 10 and K_i
256 was estimated from equation 1 (*46*). The colorimetric SSAT assay was also performed in a
257 96-well plate where enzyme activity was monitored in the presence of the respective
258 inhibitor across 8 concentrations of substrate and data were fit to a competitive inhibition
259 model in Graphpad Prism 10.

260 Equation 1: $IC_{50} = K_i\ (1+ \frac{[S]}{Km})$

261

262 **Macrophage infections.** RAW-264.7 cells were seeded ($1x10^6$ cells/mL) in RPMI
263 (Sigma Aldrich) supplemented with 10% fetal bovine serum (Fisher Scientific), 1 mM
264 HEPES (Thermofisher), and 100X MEM non-essential amino acids solution (Thermofisher)
265 in 24-well plates 2 days prior to infection and incubated at 37°C and 5% CO_2. *S.*
266 Typhimurium 14028s and *speG*::Cm were grown in appropriate selection for 16 h at 37°C.
267 Bacteria were subcultured in LB with no antibiotics until late log phase. The OD_{600} was
268 normalized and cells washed with fresh media, 10 μL of washed cells were added to 1 mL
269 of supplemented RPMI and 50 μL of the diluted bacteria was added to each well. Plates
270 were centrifuged at 1000 rpm for 1 minute and incubated at 37°C, 5% CO_2 for 10 minutes to
271 complete infection. Media was replaced (1 mL/well) at ten minutes post-infection, with
272 supplemented RPMI + 100 μg/mL gentamicin for 30 minutes to kill extracellular bacteria.
273 After 30 minutes, fresh RPMI media supplemented with 10 μg/mL gentamicin with and
274 without 10 μM OES2-0017 was added. Plates were then incubated for 4 hours. The pre-
275 infection group were treated with 10 μM OES2-0017 30 minutes prior to infection with *S.*
276 Typhimurium. Cells were lysed by washing twice with 1 mL 1X PBS and then adding 1 mL
277 1% PBS-Triton for 5 minutes per well. Lysed cells were diluted and plated on LB agar and
278 incubated at 37°C for 16 hours. Cells were lysed and plated at time 0, 4 hours post-
279 infection, and 15 hours post-infection.

280 **Phylogenetic analysis.** Protein BLAST analysis was used to identify proteins with
281 homology to *S. aureus* SpeG. Sequences were downloaded in FASTA format and a multiple
282 sequence alignment was generated using MUSCLE. A phylogenetic tree was constructed
283 using a neighbor joining method using MEGA11 and visualized using iTOL.
284 **Docking and 3D Protein Homology.** The ligand protein docking was done using
285 SwissDock (https://www.swissdock.ch/) and the docking results were visualized using
286 UCSF Chimera-1.17.3 (https://www.cgl.ucsf.edu/chimera/). The interacting amino acid
287 residues of the target protein were further illustrated by BIOVIA Discovery Studio Visualizer
288 (https://www.3ds.com/products/biovia/discovery-studio/visualization). 3D homology and
289 alignments between different proteins were performed by PyMOL 3.0
290 (https://www.pymol.org/).

291 **Results and Discussion**

292 **A high-throughput chemical screen identifies potential polyamine**
293 **detoxification inhibitors.** To identify inhibitors of polyamine detoxification mechanisms, we
294 undertook two screens against *S. aureus* USA300. In an unbiased approach, we screened
295 a library of 2560 small molecules (Spectrum collection, MicroSource Discovery Systems,
296 Inc.), comprised of previously approved drugs and natural product derivatives, at 20 μM in
297 the presence of ¼th the minimum inhibitory concentration (MIC) of spermine against
298 USA300. In parallel, we took a rationale-based approach by assembling a collection of 83
299 polyamine analogs with at least 60% structural similarity to substrates and products of
300 polyamine biosynthesis and detoxification enzymes in bacteria, reasoning that such analogs
301 have a higher probability of interacting with, and potentially inhibiting, the polyamine-related
302 enzymes of interest. Notably, several polyamine biosynthesis inhibitors are analogous to
303 natural polyamines or substrates of their biosynthetic enzymes (*47-49*), which supports this
304 rationale-based approach. We screened the polyamine analog library at 20 μM (similar to
305 the Spectrum collection screen) in the presence of spermine at ¼th the MIC. The screen
306 was performed with the hypothesis that a compound inhibiting polyamine detoxification
307 would exhibit synergy with spermine. Combined, the screens resulted in 187 primary hits
308 showing at least 80% growth inhibition. We then excluded known antimicrobials in the
309 Spectrum collection yielding 129 hits (Figure 1 A and B). We tested these hits in follow-up
310 dose-response assays in the presence and absence of a single spermine concentration
311 (Supplementary Fig. 1); only 8 compounds showed a reduction in MIC in the presence of

spermine (Figure 1A). We then tested these eight compounds in checkerboard assays with spermine; six compounds, OES1-1087, OES1-0507, OES1-1639, OES1-1238, OES2-0052, and OES2-0017, showed synergy with spermine (Figure 1C-H). Synergy was determined by calculating the fractional inhibitory concentration index (FICI), with an FICI value ≤ 0.5 defined as a synergistic interaction. OES1-1087 exhibited the strongest synergistic interaction with spermine with an FICI value of 0.15 ± 0.03 followed by OES1-0507 (0.28 ± 0.07), OES2-0017 (0.33 ± 0.06), OES1-1639 (0.42 ± 0.06), OES1-1238 (0.46 ± 0.12), and finally OES2-0052 (0.50 ± 0) (Figure 1 C-H). OES1-0507, OES1-1087, and OES1-1639 are benzenediols, OES1-1238 is an acridine, and OES2-0052 and OES2-0017 are amines. In addition to synergizing with polyamines, the six hits exhibited growth inhibitory effects against USA300 with OES2-0017 being the most potent at an MIC of 20 μM (Figure 1C-H). Of note, we prioritized OES2-0017 and OES1-1087 (isoproterenol) for further characterization based on their relative potencies (spermine synergy at FICI<0.35) and as representatives of different chemical classes (polyamine and catechols, respectively). We confirmed the structures of the two prioritized compounds by NMR (Supplementary Fig.2).

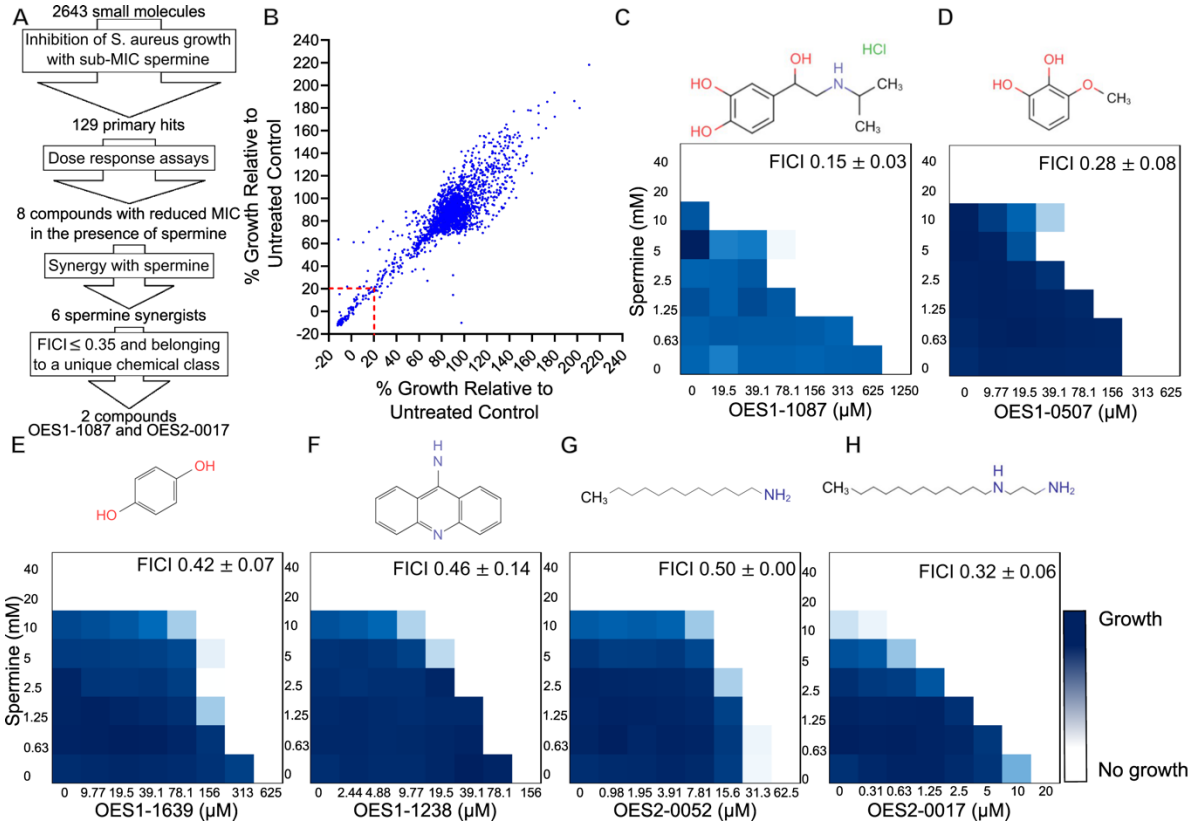

Figure 1. **High throughput screening identifies potent spermine synergists. A)** Workflow undertaken to identify chemical inhibitors of polyamine resistance. **B)** Replica plot of chemical screens performed to identify inhibitors of polyamine detoxification in *S. aureus* USA300. **C-H)** Chemical structures and

representative checkerboard assays of the hits OES1-1087 (n=9) **(C)**, OES1-0507 (n= 4) **(D)**, OES1-1238 (n=3) **(E)**, OES1-1639 (n=3) **(F)**, OES2-0052 (n=3) **(G)**, and OES2-0017 (n=11) **(H)** with spermine against *S. aureus* USA300. FICI values are reported as mean ± standard deviation of the indicated number of replicates.

A chemogenomic screen to uncover the putative mechanism of spermine synergy. We undertook a genome-wide approach to identify the putative mechanism of spermine synergy by the screen hits, reasoning that a mutant with disruption in their putative target would exhibit both increased spermine susceptibility and loss or reduction in spermine-hit compound synergy. First, we sought to uncover the determinants of polyamine detoxification whose mutants would exhibit increased susceptibility to spermine by screening the Nebraska Transposon Mutant Library (NTML), a sequence-defined transposon mutant library covering the non-essential genome of *S. aureus* USA300 (*39*), against spermine at 1/8th and 1/16th the wild-type MIC. *speG*::Tn was sensitized to spermine, in agreement with previous reports (*19*), thus serving as an internal control for the screen. Mutants in another four determinants not previously linked to the response to polyamines, *tcaA*::Tn, *cls*::Tn, *prmC*::Tn, and *pyrP*::Tn, were also sensitized to spermine (Figure 2 A). Dose-response assays showed an 8-fold reduction in spermine MIC in *speG*::Tn, and a decrease of the other four mutants at ½ MIC relative to the wild-type strain (Supplementary Fig. 3). We constructed an in-frame unmarked deletion of *speG* given that its transposon mutant had the most pronounced spermine MIC shift; Δ*speG* confirmed the observed spermine susceptibility shift (Supplementary Fig. 3). *tcaA* encodes a predicted transmembrane protein and is implicated in teicoplainin resistance (*50*). *cls* encodes a cardiolipin synthase involved in modulating the phospholipid composition of the membrane (*51*). *prmC* encodes a release factor methyltransferase, and *pyrP* an uracil-xanthine permease. The molecular basis linking these determinants to polyamine response warrants further investigation, which falls beyond the scope of this study. Notably, *sbnB*::Tn, disrupted in a gene encoding an enzyme involved in the siderophore staphyloferrin B biosynthesis (*52*), was initially identified in the screen and showed an 8-fold spermine MIC reduction; however, Δ*sbnB* mutant was not sensitized to spermine (Supplementary Fig. 3). Whole-genome sequencing and subsequent PCR analysis of the *sbnB*::Tn mutant revealed an additional truncation of 46.8 kb comprising the SCC*mec* cassette and the ACME locus, including *speG* and *mecA* (Supplementary Fig. 3); hence, *sbnB* was excluded from the putative determinants list.

365 Next, we resupplied the hit compounds and conducted mini-checkerboard assays
366 with spermine against the five identified polyamine resistance determinants to detect loss or
367 reduction in synergy. The spermine synergistic interaction with OES2-0017 and OES1-1087
368 was lost or reduced in the Δ*speG* mutant (Figure 2 B), suggesting that SpeG is the putative
369 target of these compounds. Notably, spermine synergy was also lost in the other four de-
370 prioritized hit compounds against *ΔspeG* mutant (Supplementary Fig. 4), suggesting that all
371 six hits uncovered from the screens share a similar molecular target for spermine synergy.
372 We performed checkerboard assays with spermine and OES2-0017 or OES1-1087
373 against other *speG*$^{+}$ and *speG*$^{-}$ *S. aureus* strains. The tested strains included another
374 USA300 strain CMRSA-10 that encodes *speG* as well as two strains that do not encode
375 *speG* including the MRSA strain COL and the methicillin-sensitive *Staphylococcus aureus*
376 (MSSA) strain NCTC8325. The *speG*$^{-}$ strains, whether MRSA or MSSA, displayed a loss or
377 reduction in synergy between spermine and OES2-0017 or OES1-1087, phenocopying the
378 USA300 *ΔspeG* mutant (Figure 2 C-H). For both OES2-0017 and OES1-1087, CMRSA-10
379 displayed a similar synergistic phenotype to that observed in the other wild-type USA300
380 strain, JE2 (Figure 2 I and J). These results further suggest that OES2-0017 and OES1-
381 1087 are inhibiting SpeG activity, and that strains must encode *speG* to observe the
382 spermine synergistic phenotype.
383 Since SpeG is a spermine/spermidine acetyltransferase, we also tested spermidine
384 with either OES2-0017 or OES1-1087 in checkerboard assays. As expected, OES2-0017
385 and spermidine synergized with an FICI of 0.33 $\pm$ 0.06, such synergy was decreased in the
386 *ΔspeG* mutant (FICI = 0.48 $\pm$ 0.05) and *speG*$^{-}$ strains but not completely lost (Figure 2 K
387 and L and Supplementary Fig. 5). The same is observed with spermidine and OES1-1087
388 where the Δ*speG* mutant (FICI = 0.38 $\pm$ 0.09) or *speG*$^{-}$ strains showed reduced synergy
389 compared to wild-type USA300 (FICI = 0.17 $\pm$ 0.03) (Figure 2 M and N and Supplementary
390 Fig. 5). The results suggest that synergy between these compounds and spermidine is
391 mediated, at least in part, by SpeG inhibition.
392
393 **SpeG as the target of OES1-1087 and OES2-0017**. We sought to confirm the
394 SpeG inhibitory activity of the hit compounds in *in vitro* assays using purified His-tagged
395 recombinant SpeG. We used a colorimetric SSAT assay based on the quantification of
396 CoA-SH formed during the transfer of the acetyl group from acetyl-CoA, which is
397 proportional to the amount of the acetylated substrate (AcCoA) (*45*). Under these

398 experimental conditions, we observed acetyltransferase activity for the native and not the
399 heat-inactivated SpeG when both spermine and spermidine were used as the test
400 substrates. Based on our results and previous analysis(*53*), SpeG displays Michaelis-
401 Menten kinetics with spermine as a substrate, allosteric kinetics with spermidine, and no
402 activity with putrescine, thus we estimated catalytic efficiency of each as K_m and $S_{0.5}$,
403 respectively. The SpeG K_m with spermine was 1312 $\pm$ 348.1 μM and $S_{0.5}$ with spermidine
404 was 8669 $\pm$ 3031 μM (Supplementary Fig. 6). Catalytic efficiency of SpeG with spermine
405 and spermidine as substrates were 5.58E+03 and 2.51E+02 $M^{-1}s^{-1}$, respectively
406 (Supplementary Fig. 6). These results agree with previous reports showing that spermine is
407 the preferred substrate of SpeG, followed by spermidine and that SpeG does not acetylate
408 putrescine (*20, 53*).

409 Next, we confirmed that OES2-0017 and OES1-1087 inhibited acetyltransferase
410 activity of SpeG *in vitro* by performing enzymatic inhibition assays testing a dilution series of
411 each of the hits in the presence of either a single concentration or multiple concentrations of
412 substrate in a checkerboard-style format estimating IC_{50} and K_i, respectively. The IC_{50} of
413 OES2-0017 against SpeG was 34.82 $\pm$ 6.810 μM at ~ 1 x K_m of spermine and the K_i was
414 20.20 $\pm$ 3.446 μM when varying spermine concentrations both at a fixed saturating AcCoA
415 concentration (Figure 2 O and Supplementary Fig 7). The IC_{50} of OES1-1087 was 5508 $\pm$
416 1890 μM (at ~1 x K_m of AcCoA and a spermine ~ 1 x K_m concentration; Figure 2 P). OES1-
417 1087 did not exhibit inhibitory activity under a fixed AcCoA concentration and variable
418 spermine concentrations; however, at a fixed spermine concentration and variable AcCoA,
419 OES1-1087 inhibited SpeG with an estimated K_i of 5153 $\pm$ 2126 μM (Supplementary Fig.
420 8). K_i calculations were based on fitting the checkerboard-style data to the competitive
421 inhibition model for both inhibitors, which was further supported by Lineweaver-Burk
422 transformations (Supplementary Fig. 7 and 8). These values are slightly higher than
423 expected when compared to the concentrations exhibiting spermine synergy interactions in
424 whole-cell assays. However, this could be attributed to the *in vitro* cell-free experimental
425 conditions (i.e., buffer concentration, pH, temperature, etc.) that do not perfectly match the
426 conditions *in vivo,* which may be more optimal for catalysis. Of note, we use a high buffer
427 concentration (100 mM Tris-HCl) to prevent polyamine high pH-mediated cleavage of
428 Ellman's reagent, which is sensitive to high pH (*54*). These data confirm that both OES2-
429 0017 and OES1-1087 inhibit SpeG with OES2-0017 being more potent as a SpeG inhibitor,

430 matching with the whole-cell assay results (Figure 2 O and P and Supplementary Fig. 7 and
431 8).
432 *S. aureus* SpeG forms a dodecameric structure composed of two hexamers stacked
433 together in a ring-like structure (*53*). Crystallographic data of SpeG from *S. aureus*, *Vibrio*
434 *cholerae*, and *E. coli* show spermine and spermidine bound in a pocket that expands two
435 adjacent monomers of the hexamer with a total of twelve binding sites in the dodecamer
436 (*53, 55, 56*). When spermine, spermidine, or AcCoA bind to SpeG a conformational change
437 occurs, suggested to bring the AcCoA and polyamine molecule closer together for the
438 acetyl transfer (*53, 55, 57, 58*). Alignment of the crystal structures of *S. aureus* SpeG with
439 and without bound spermine depicts this conformational change and the spermine binding
440 site (PBD ID: 8FV0 and 5IX3, respectively; Figure 2 Q). We docked both OES2-0017 and
441 OES1-1087 in an unbiased manner to *S. aureus* SpeG (PBD ID: 5IX3). OES2-0017 is
442 predicted to bind between adjacent monomers at the same site as spermine and spermidine
443 with a ΔG of -6.636 Kcal/mol (Figure 2 R). This analysis aligns with our experimental data,
444 suggesting OES2-0017 is a competitive inhibitor of SpeG, competing with spermine to bind
445 the free enzyme.
446 *S. aureus* SpeG has not been crystalized in complex with CoA or AcCoA, but *V.*
447 *cholerae* SpeG has been co-crystallized with CoA, where it binds to the substrate binding
448 site between a cleft created by β4 and β5 strands and α-helices 3 and 4 (*55*). Molecular
449 docking of *S. aureus* SpeG with AcCoA predicts it binds to the same site as in *V. cholerae*
450 (ΔG of -9.228 Kcal/mol; Figure 2 S). OES1-1087 was also predicted to bind this same
451 location (ΔG = -6.691 Kcal/mol; Figure 2 T). This prediction combined with our experimental
452 inhibition data led us to hypothesize that OES1-1087 is binding the same site as AcCoA and
453 is thus suggested to be acting as a competitive inhibitor. The lower affinity of OES1-1087 to
454 bind to the same site as AcCoA also suggests why OES1-1087 shows very weak inhibition
455 of SpeG. The *in vitro* enzymatic assays and protein docking data together suggest that
456 OES2-0017 and is OES1-1087 are competing with spermine or AcCoA, respectively to bind
457 SpeG, acting in a competitive manner.
458

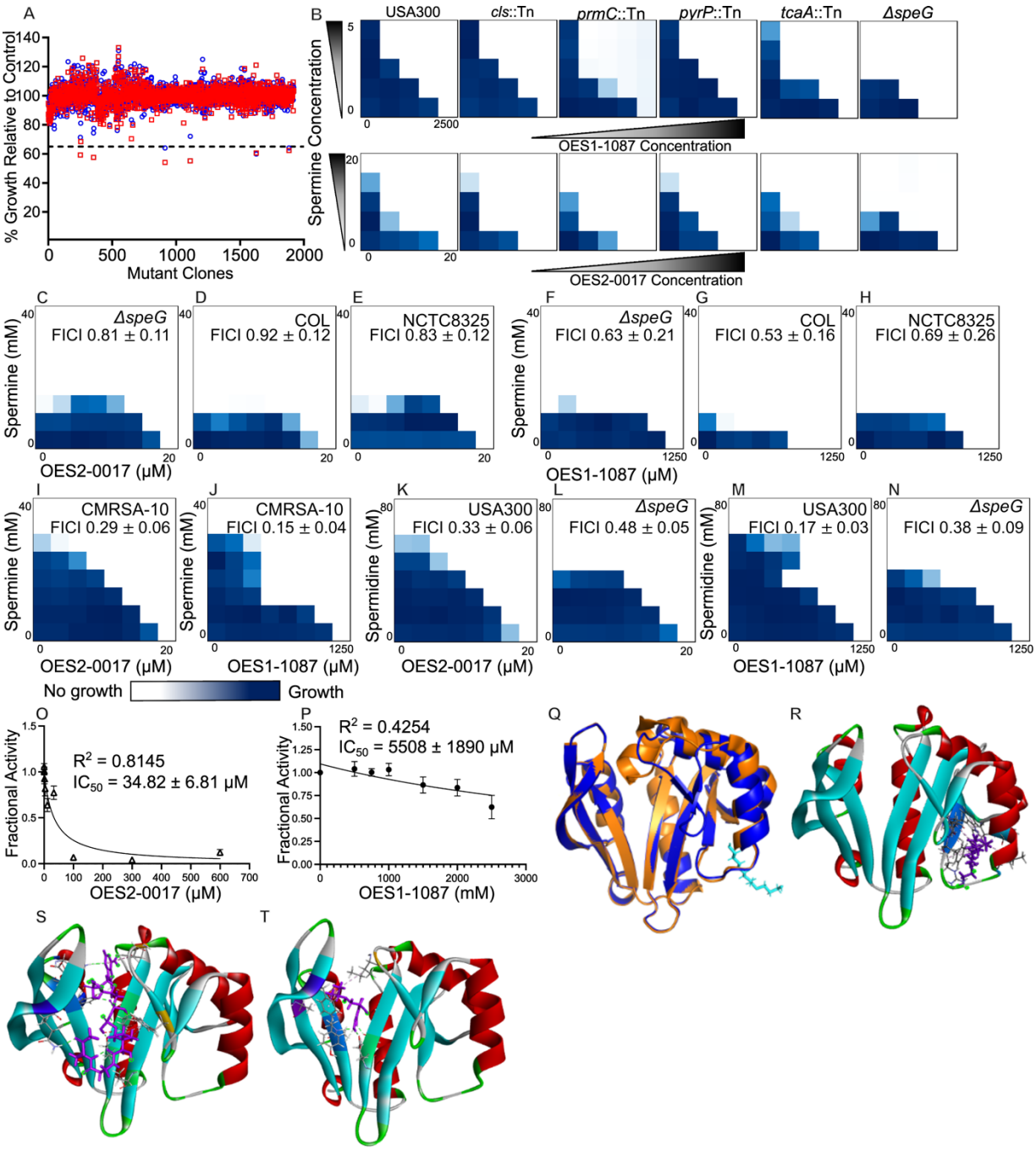

Figure 2. **OES2-0017 and OES1-1087 inhibit SpeG. A)** Chemogenomic screen of the Nebraska Transposon Mutant Library with spermine at 1/8th (red squares) and 1/16th (blue circles) the MIC. **B)** Mini-checkerboard assays performed by testing 2-fold dilutions of each of spermine and OES1-1087 or OES2-0017 against polyamine resistance determinants uncovered in **(A)** including *S. aureus* USA300, *cls*::Tn, *prmC*::Tn, *pyrP*::Tn, *tcaA*::Tn, and Δ*speG*. **C-N)** Representative checkerboard assays performed by testing 2-fold dilutions of each test compound. **C-E)** spermine and OES2-0017 against *S. aureus* Δ*speG* (n=9) **(C)**, COL (n=3) **(D)**, NCTC8325 (n=3) **(E)**. **F-H)** Spermine and OES1-1087 against *S. aureus* Δ*speG* (n=9) **(F)**,

467 COL (n=4) **(G)**, NCTC8325 (n=4) **(H)**. **I)** OES2-0017 and spermine against CMRSA-10 (n=3), **J)** OES1-
468 1087 and spermine against CMRSA-10 (n=3). OES2-0017 and spermidine against **K)** USA300 (n=7) and
469 **L)** Δ*speG* (n=6). OES1-1087 and spermidine against **M)** USA300 (n=3) and **N)** Δ*speG* (n=3).
470 Checkerboards against Δ*speG* were performed on the same day as their counterparts against the wild-type
471 strain shown in Figure 1. **O-P)** Colorimetric enzymatic assays conducted with 1 mM Acetyl Coenzyme A
472 **(O)** or 0.75 mM Acetyl Coenzyme A **(P)** and 1500 μM spermine in the reaction mixture to evaluate the
473 inhibition of OES2-0017 (n=7; **O)** and OES1-1087 (n=3**; P).** Data is represented as mean ± SEM for three
474 independent experiments. **Q)** Alignment of *S. aureus* SpeG crystallized with (orange; PDB ID: 8FV0) and
475 without spermine (blue; PDB ID 5IX3). Molecular docking of **R)** OES2-0017, **S)** Acetyl-CoA, and **T)** OES1-
476 1087 to *S. aureus* SpeG (PDB ID: 5IX3).
477
478 **Uncovering parallel polyamine acetyltransferase mechanisms in USA300.**
479 Checkerboard assays with OES2-0017 and OES1-1087 revealed only a partial loss of
480 synergy in the Δ*speG* mutant with the polyamine spermidine (Figure 2 K-N and
481 Supplementary Fig. 5), suggesting other potential mechanisms may also be at play in the
482 spermidine synergy and that these may also be targeted by the inhibitors. SpeG
483 preferentially acetylates spermine while it acetylates spermidine with a lower affinity
484 (Supplementary Fig. 5 and (*20, 53*)). The lower affinity may contribute to a decreased ability
485 to detoxify spermidine, possibly requiring other detoxification mechanisms that function in
486 parallel to SpeG. Some bacteria encode SSATs distinct from SpeG, such as *B. subtilis*
487 encoding two enzymes *paiA* and *bltD* (*59, 60*) and *Enterococcus faecalis* encoding *pmvE* a
488 homolog of *B. subtilis paiA* (*25, 59, 60*). The presence of both *paiA* and *bltD* in *B. subtilis*
489 provides evidence for the existence of parallel polyamine detoxification pathways. Further, a
490 recent report observed an accumulation of *N*-acetylputrescine in the MSSA strain ATCC
491 25923, which does not encode SpeG; however, they did not identify the enzyme
492 responsible for its production (*21*). This further suggests that *S. aureus* may encode
493 alternative polyamine acetyltransferases and that they may have activity towards different
494 polyamines. We identified potential additional polyamine acetyltransferases in *S. aureus* by
495 performing protein blast of the *B. subtilis* 168 strain sequences of BltD (Accession
496 NP_390537.1) and PaiA (Accession NP_391095.1) against *S. aureus* to identify potential
497 homologs. Blastp results for BltD revealed two hypothetical proteins of *S. aureus* USA300
498 FPR3757; SAUSA300_0441 with 29.76 percent identity (query coverage 54%, E value of
499 $2e^{-09}$) and SAUSA300_2083 with 27.41 percent identity (query coverage 86%, E value of
500 $5e^{-09}$). PaiA blastp results identified a homolog of *S. aureus* USA300 FPR3757;

501 SAUSA300_2316 (denoted $PaiA_{Sa}$ herein), with 40.35 percent identity (99% query
502 coverage, E value of 3 e^{-39}). These *S. aureus* proteins have not been previously
503 characterized functionally; all three are annotated as ribosomal-protein-alanine
504 acetyltransferases whereas SAUSA300_2083 and SAUSA300_2316 ($PaiA_{Sa}$) are also
505 annotated as spermine/spermidine acetyltransferase blt and PaiA, respectively.
506 To confirm or rule out SSAT activity of SAUSA300_2083, SAUSA300_0441, and
507 $PaiA_{Sa}$, we overexpressed and purified these enzymes to assess their activity *in vitro*. We
508 observed acetyltransferase activity of $PaiA_{Sa}$ when spermine and spermidine are used as
509 substrates but no activity with putrescine under the test conditions (Figure 3
510 A-C). $PaiA_{Sa}$ substrate affinity appears higher for spermine than spermidine (K_M = 2144 $\pm$
511 443.3 μM and 3996 $\pm$ 670.8 μM, respectively). Further, the catalytic efficiency of $PaiA_{Sa}$
512 with spermine as a substrate is ~7-fold higher than with spermidine (K_{cat}/K_M = 2.41E+03 and
513 3.47E+02 $M^{-1}s^{-1}$, respectively; Supplementary Fig. 9). Thus, these results suggest that
514 $PaiA_{Sa}$ is better at acetylating spermine at lower substrate concentrations than spermidine.
515 Notably, SAUSA300_2083 and SAUSA300_0441 did not exhibit actetyltransferase activity
516 against the polyamines spermine, spermidine or putrescine under the tested conditions
517 (Supplementary Fig. 9). These data suggest that the $PaiA_{Sa}$ is likely to function as a
518 spermine/spermidine acetyltransferase. Next, we tested the ability of OES2-0017 to inhibit
519 $PaiA_{Sa}$ spermine acetylation; the low spermidine acetylation signal precluded testing OES2-
520 0017 $PaiA_{Sa}$ inhibition with spermidine as a substrate. OES2-0017 inhibited $PaiA_{Sa}$ activity
521 exhibiting an IC_{50} value of 52.17 $\pm$ 5.897 μM and estimated K_i of 43.83 $\pm$ 6.693 (Figure 3 D
522 Supplementary Fig. 10). Next, we performed whole-cell spermine – OES2-0017 mini-
523 checkerboard assays against a *paiA*::Tn mutant, compared to the wild-type USA300,
524 revealing no loss of synergy in the *$paiA_{Sa}$* mutant (Figure 3 E and F). SpeG, hypothesized to
525 be the primary spermine/spermidine detoxification enzyme in *S. aureus*, may have
526 compensated for the absence of $PaiA_{Sa}$, masking any phenotypic changes in the *$paiA_{Sa}$*
527 mutant; a *speG $paiA_{Sa}$* double mutant may be required to assess the contribution of $PaiA_{Sa}$
528 in whole cells. Together, our results indicate that polyamine acetylation in *S. aureus* may
529 occur through $PaiA_{Sa}$ in addition to SpeG, serving as complementary acetyltransferase
530 enzymes, and that the SSAT function of both enzymes is inhibited by OES2-0017.

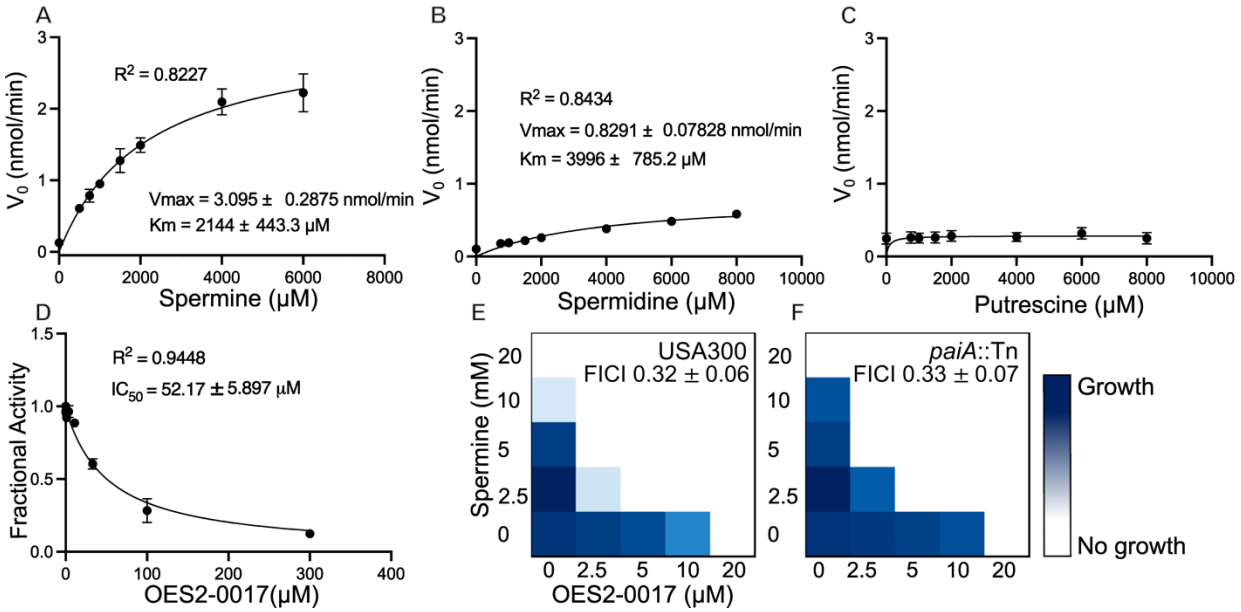

Figure 3. **Interaction of polyamines and OES2-0017 uncovers PaiA$_{Sa}$ as a spermine/spermidine acetyltransferase in *S. aureus*. A-C)** Steady-state enzymatic assays of PaiA$_{Sa}$ evaluate the acetylation activity in the presence of substrates **A)** spermine (n=6), **B)** spermidine (n=6), and **C)** putrescine (n=6). **D)** Enzymatic inhibition assay of PaiA$_{Sa}$ with spermine as a substrate by OES2-0017 (n=3). Results are represented as a mean ± SEM of three independent experiments. Representative checkerboard assays of spermine and OES2-0017 against *S. aureus* **E)** USA300 (n=11), **F)** *paiA*::Tn (n=3). FICI values are represented as mean ± standard deviation.

Uncovering the mechanism of growth inhibitory effects of OES2-0017. OES2-0017 and OES1-1087 exhibit growth-inhibitory effects at concentrations higher than those required to synergize with spermine; therefore, we hypothesized that this activity occurs via a second mode of action. Given its growth inhibitory activity at low micromolar range, we prioritized OES2-0017 to determine if growth inhibition was mediated through an essential protein target. We confirmed activity against *Bacillus subtilis,* a Gram-positive organism with high degree of genetic conservation with *S. aureus* (Supplementary Fig. 11). Then, we screened a knock-down library covering the essential genes of *B. subtilis* against three sub-inhibitory concentrations of OES2-0017, spanning ¼th-1/16th the wild-type MIC (Supplementary Fig. 11). While some mutants showed reduced growth in the presence of one or more of the tested sub-inhibitory concentrations, follow-up dose-response assays revealed that none of those mutants was more susceptible to OES2-0017 relative to the wild-type, suggesting the absence of an essential protein target.

Next, we hypothesized that the growth-inhibitory activity of OES2-0017 is due to an effect on membrane integrity in the absence of an essential protein target. Using a $DiSC_3(5)$

555 membrane integrity assay (*43*), we found that OES2-0017 permeabilized the membrane of
556 USA300 at concentrations starting from its MIC (≥ 20 μM) in a concentration-dependent
557 manner (Figure 4 A and B), suggesting membrane activity at high concentrations as the
558 mechanism of growth inhibitory effects of OES2-0017. Notably, a $DiSC_3(5)$ assay with
559 OES1-1087 did not have an observable effect on membrane integrity (Figure 4 C).

560 Next, we sought to check whether membrane disruption contributed to the observed
561 synergy between OES2-0017 and spermine. We conducted a checkerboard-style $DiSC_3(5)$
562 assay with a combination of spermine and OES2-0017. OES2-0017 concentrations that
563 correspond to the range of synergy (2.5-10 μM) resulted in no observable permeabilization
564 (Figure 4 A and B). Like OES2-0017, spermine disrupted membrane integrity of USA300 at
565 concentrations starting from its MIC against USA300 (Figure 4 B and Supplementary Fig.
566 12 A). We observed the similar membrane permeabilization with spermidine and putrescine
567 (Supplementary Fig. 12 B and C) Large polyamine molecules were previously shown to
568 permeabilize the outer membrane of Gram-negative bacteria (*61*); however, we found no
569 reports on similar effects on Gram-positive membrane integrity. Importantly, there was no
570 significant effect on membrane integrity in the presence of the combination of OES2-0017
571 and spermine at concentrations where synergy is observed (Figure 4 B), suggesting that
572 membrane permeabilization does not contribute to the observed synergy. Taken together,
573 we revealed a dual mode of action of OES2-0017 with high concentrations leading to
574 growth-inhibitory effects due to membrane perturbation and low concentrations synergizing
575 with polyamines through inhibiting SpeG and other SSAT activity.

576

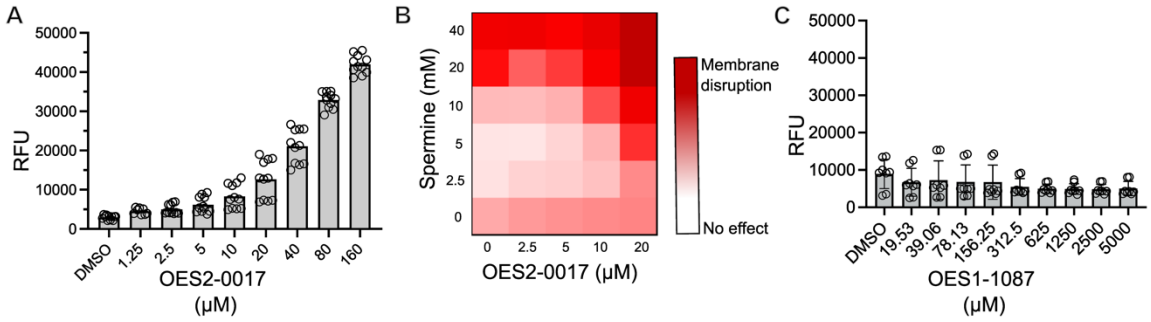

577

578 Figure 4. **Effects of OES2-0017 and OES1-1087 on *S. aureus* membrane integrity. A)** $DiSC_3(5)$
579 membrane permeabilization assay of OES2-0017 against *S. aureus* USA300. Results represented as mean
580 relative fluorescence units (RFU) ± SEM for three independent experiments (n=11). **B)** A representative
581 $DiSC_3(5)$ membrane permeabilization assay performed as a mini-checkerboard evaluating the combined
582 effects of OES2-0017 and spermine. **C)** $DiSC_3(5)$ membrane permeabilization assay of OES1-1087 against
583 *S. aureus* USA300. Results represented as mean ± SEM for three independent experiments (n=8).

584

585 **Broad-spectrum activity of OES2-0017 on clinically-relevant bacteria.** We conducted a
586 BLAST search of spermine/spermidine acetyltransferases using *S. aureus* SpeG as the
587 query, obtaining 94 amino acid sequences comprising eukaryotes, bacteria, and archaea.
588 Sequences were aligned using MUSCLE and a pairwise deletion of ambiguous positions
589 was performed for each sequence pair. The conservation of various SSATs was determined
590 by a maximum likelihood phylogenetic analysis (Supplementary Fig. 13). Although the main
591 purpose of such an analysis is to infer evolutionary history and relatedness, we used the
592 phylogenetic tree to visualize or infer sequence similarity between known
593 spermine/spermidine acetyltransferases. Our analysis reveals two main branches
594 originating from a common ancestor. The first branch shows archaea and (vertebrate)
595 eukaryotic organisms clustering together. This branch includes the human SAT1, rat, and
596 other mammalian SATs. The same branch also included *Acinetobacter baumannii* Dpa,
597 which was recently characterized as more closely resembling eukaryotic SSATs than
598 bacterial ones (*62*). The second branch was divided into two sub-branches; the first
599 contained SpeG homologs in yeast while the second large sub-branch comprised bacterial
600 SpeG. The latter sub-branch included SpeG and other polyamine acetyltransferases that
601 have previously been characterized in both Gram-positive and Gram-negative organisms
602 including *Staphylococcus epidermidis* (*23*)*, E. faecalis* (PmvE) (*25*), *Escherichia coli* (*63*)*, V.*
603 *cholerae* (*55*)*, Yersinia pestis* (PDB ID: 6D72)*, B. subtilis* (BltD and PaiA) (*59, 60*)*,* and
604 *Salmonella enterica* serovar Typhimurium (*24*).

605 Given that SpeG has been implicated in virulence phenotypes in multiple bacteria
606 (*14, 24, 64*), we tested OES2-0017 being the most potent identified SpeG inhibitor against a
607 broad range of Gram-positive and Gram-negative bacteria and the pathogenic yeast
608 *Candida albicans* in checkerboard assays with spermine. The combination of OES2-0017
609 and spermine exhibited a synergistic interaction or an increase in spermine susceptibility in
610 *B. subtilis, E. faecalis, E. faecium, S. epidermidis, M. smegmatis, B. cenocepacia, E. coli, K.*
611 *pneumoniae, S.* Typhimurium, and *C. albicans* (Figure 5 A-K)*.* In *A. baumannii* the
612 polyamine acetyltransferase Dpa preferentially acetylates 1,3-diaminopropane (*62*), which is
613 a diamine; therefore, we tested the diamine putrescine and OES2-0017 in combination.
614 OES2-0017 synergized with putrescine against *A. baumannii* (Figure 5 K). As in *S. aureus*,
615 OES2-0017 also inhibited the growth of all tested bacteria and *C. albicans* at the micromolar

range (Figure 5). Next, we tested the combination of spermine and OES2-0017 against the respective SSAT mutants of *E. coli* BW25113, *K. pneumoniae* MKP103, *S. enterica* sv. Typhimurium 14028s, and *B. subtilis* 168 (Figure 5. L-O). OES2-0017 no longer potentiated the effects of spermine in the SSAT mutants as opposed to their respective wild-type strains (Figure 5 L-O), suggesting OES2-0017 mediates its broad-spectrum spermine synergy through SSAT inhibition. Together, OES2-0017 exhibited broad-spectrum dual activity – polyamine synergy and growth inhibition – against Gram-positive and Gram-negative bacteria and fungi, including clinically relevant World Health Organization priority pathogens (*65*).

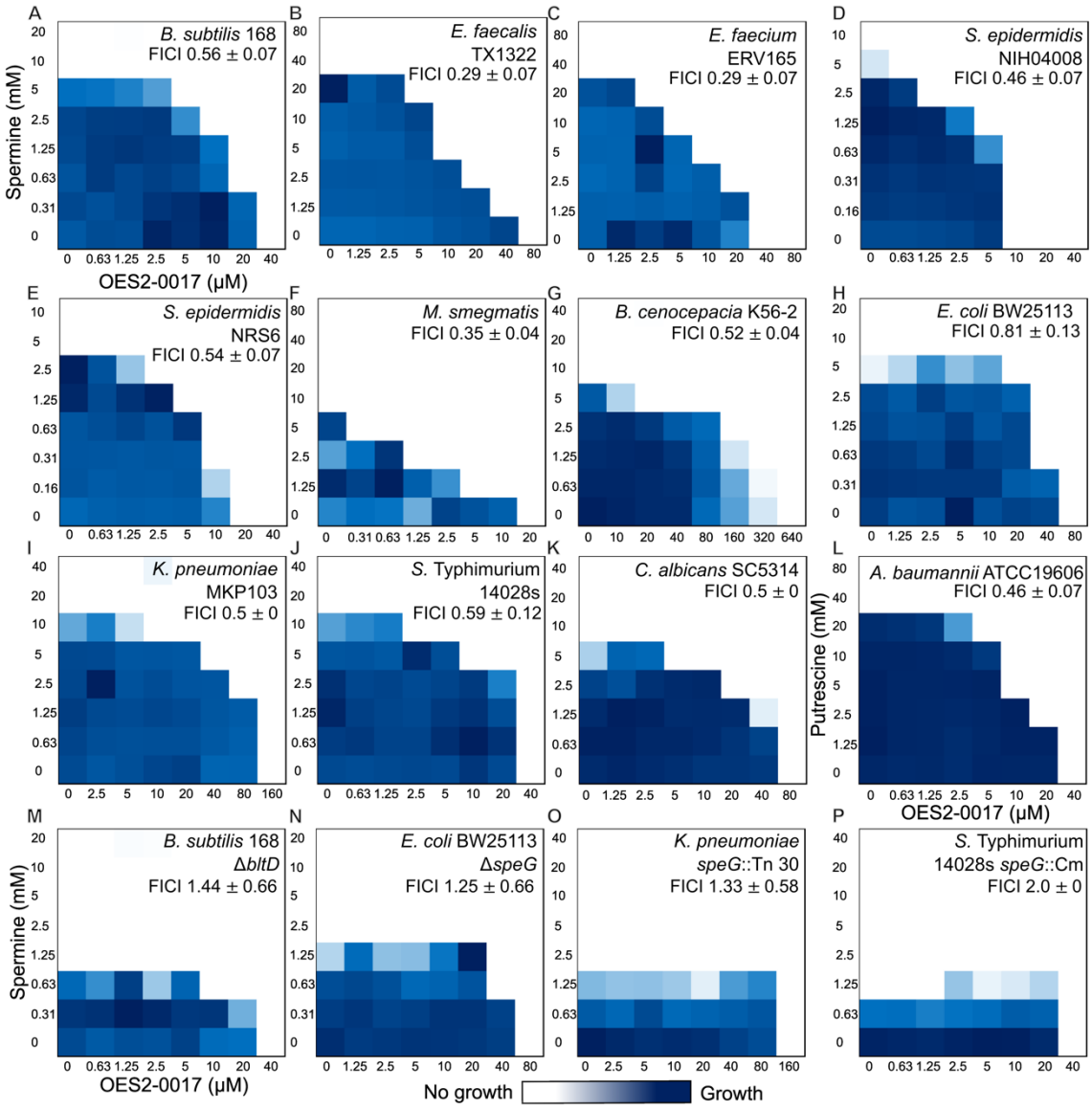

626 Figure 5. **OES2-0017 exhibits broad-spectrum activity.** Representative checkerboard assays of OES2-
627 0017 and spermine against **A)** *B. subtilis* 168 (n=4), **B)** *E. coli* BW25113 (n=4), **C)** *K. pneumoniae* MKP103
628 (n=4), **D)** *S.* Typhimurium 14028s (n=4), **E)** *E. faecalis* TX1322 (n=3), **F)** *E. faecium* ERV165 (n=3), **G)** *S.*
629 *epidermidis* NRS6 (n=3), **H)** *S. epidermidis* NIH04008 (n=3), **I)** *B. cenocepacia* K56-2 (n=3), **J)** *M.*
630 *smegmatis* (n=3), and **K)** *C. albicans* SC5314 (n=3). **L)** Putrescine and OES2-0017 checkerboard against
631 *A. baumannii* ATCC19606 (n=3). Representative checkerboard assays of spermine and OES2-0017
632 against spermine/spermidine acetyltransferase mutants **M)** *B. subtilis* Δ*bltD* (n=4), **N)** *E. coli* Δ*speG* (n=3),
633 **O)** *K. pneumoniae speG*::Tn30 (n=3), **P)** *S.* Typhimurium *speG*::Cm (n=3)**.** FICI values are represented as
634 mean ± standard deviation for the indicated number of replicates.

635
636

637 **Polyamine-mediated altered antibiotic susceptibility and the potential of OE2-0017 as**
638 **an antibiotic adjuvant.** Checkerboard assays of polyamines and representative antibiotics
639 from seven classes with diverse cellular targets revealed various polyamine-mediated
640 altered antibiotic responses (Supplementary Fig. 14). The three tested polyamines
641 synergized with the macrolide azithromycin while spermine synergized with the β-lactam
642 cefuroxime (Supplementary Fig. 14). The spermine β-lactam synergy matches previous
643 reports of the phenotype in *S. aureus* (*26, 28*). Similarly, polyamine synergy with macrolides
644 has been reported in the Gram-negative pathogens *K. pneumoniae* (*30*) and *E. coli* (*28*). In
645 *K. pneumoniae* the synergistic interaction between azithromycin and putrescine is mediated
646 through the combined effects of putrescine-induced membrane perturbation and protein
647 synthesis inhibition via interaction at the ribosome (*30*). The effects of polyamines on
648 ribosome function is well documented (*66*) and polyamines are known to interact with
649 biological macromolecules, including DNA, RNA, proteins, and phospholipids (*16, 67*). In
650 contrast, the three polyamines antagonized rifampicin and kanamycin whereas spermine
651 antagonized with vancomycin, defined as a FICI value ≥ 4 (Supplementary Fig. 14). The
652 mechanisms of the observed polyamine-mediated alterations to antibiotic susceptibility
653 warrant further investigation. On the other hand, we observed no alterations in daptomycin
654 or ciprofloxacin susceptibility in combination with the tested polyamines (Supplementary
655 Fig. 14).

656 Interestingly, the MIC of vancomycin is increased 4-fold when combined with
657 spermine (FICI = 4.69 ± 1.57), but the interaction is lost in a Δ*speG* mutant (FICI = 2.17 ±
658 0.26), suggesting that *S. aureus* requires a functional SpeG to use exogenous polyamines
659 to resist vancomycin (Figure 6 A and B). Supplementing a sub-inhibitory concentration of
660 OES2-0017 (2.5 μM) to a vancomycin-spermine checkerboard against *S. aureus* USA300
661 phenocopied the loss of antagonism observed against the Δ*speG* mutant (FICI = 1.59 ±

662 0.62; Figure 6 C). This phenotype is not due to a synergistic interaction between OES2-
663 0017 and vancomycin (Supplementary Fig. 15). Vancomycin is one of the first-line
664 antibiotics for the treatment of severe MRSA infections (*68*), suggesting the antagonism
665 between polyamines and vancomycin may be detrimental to MRSA treatment. Similarly, the
666 polyamine antagonistic interactions with rifampicin and kanamycin in USA300 were lost in
667 the Δ*speG* mutant and with supplementation of a sub-inhibitory concentration of OES2-0017
668 to the USA300 checkerboard (Figure 6 D-I). The loss of antagonism was not due to synergy
669 between OES2-0017 and kanamycin or rifampicin (Supplementary Fig. 15). While
670 kanamycin and rifampicin are not considered first-line monotherapies for MRSA infections,
671 they are often used in conjunction with vancomycin (*69, 70*); polyamines may reduce
672 bacterial susceptibility to these antibiotics. We also identified a synergistic interaction
673 between OES2-0017 and cefuroxime, where OES2-0017 lowered the MIC of the antibiotic
674 to <16 µg/mL from 1024 µg/mL (FICI = 0.35 $\pm$ 0.13; Figure 6 J). OES2-0017 and
675 azithromycin also exhibited a slight potentiation effect against USA300 (FICI = 0.72 $\pm$ 0.21;
676 Figure 6 K). A similar potentiation effect was observed, where azithromycin synergized with
677 OES2-0017 against *K. pneumoniae* (*30*). These results suggest that OES2-0017 may serve
678 as an antibiotic adjuvant by preventing *S. aureus* from utilizing exogenous polyamines to
679 resist antibiotics (e.g., glycopeptides, aminoglycosides, and rifamycins) or by potentiating
680 the effects of antibiotics phenocopying the polyamine-mediated sensitization to certain
681 antibiotics (e.g., macrolides and β-lactams).

682 **OES2-0017 abrogates intracellular survival and may serve as an antivirulence agent.**

683 We tested the ability of OES2-0017 to clear *S.* Typhimurium infection of murine
684 macrophages since SpeG was previously shown to be necessary for the intracellular
685 replication of *S.* Typhimurium, where a *speG* knockout was attenuated in macrophages
686 (*24*). Bacterial load was significantly reduced in a gentamicin protection assay at both 4-
687 and 15-hours post-infection in the *speG::*Cm infected macrophages compared to the wild-
688 type (p = 0.0286 and 0.0286, respectively; Figure 6 L and M). OES2-0017 treatment,
689 whether pre- or post-infection, reduced *S.* Typhimurium bacterial load in macrophages,
690 similar to the levels of recovered bacteria in the *speG*::Cm condition (Figure 6 L and M).
691 Thus, OES2-0017 eradicated intracellular macrophage infection of the wild-type *S.*
692 Typhimurium reducing its virulence.

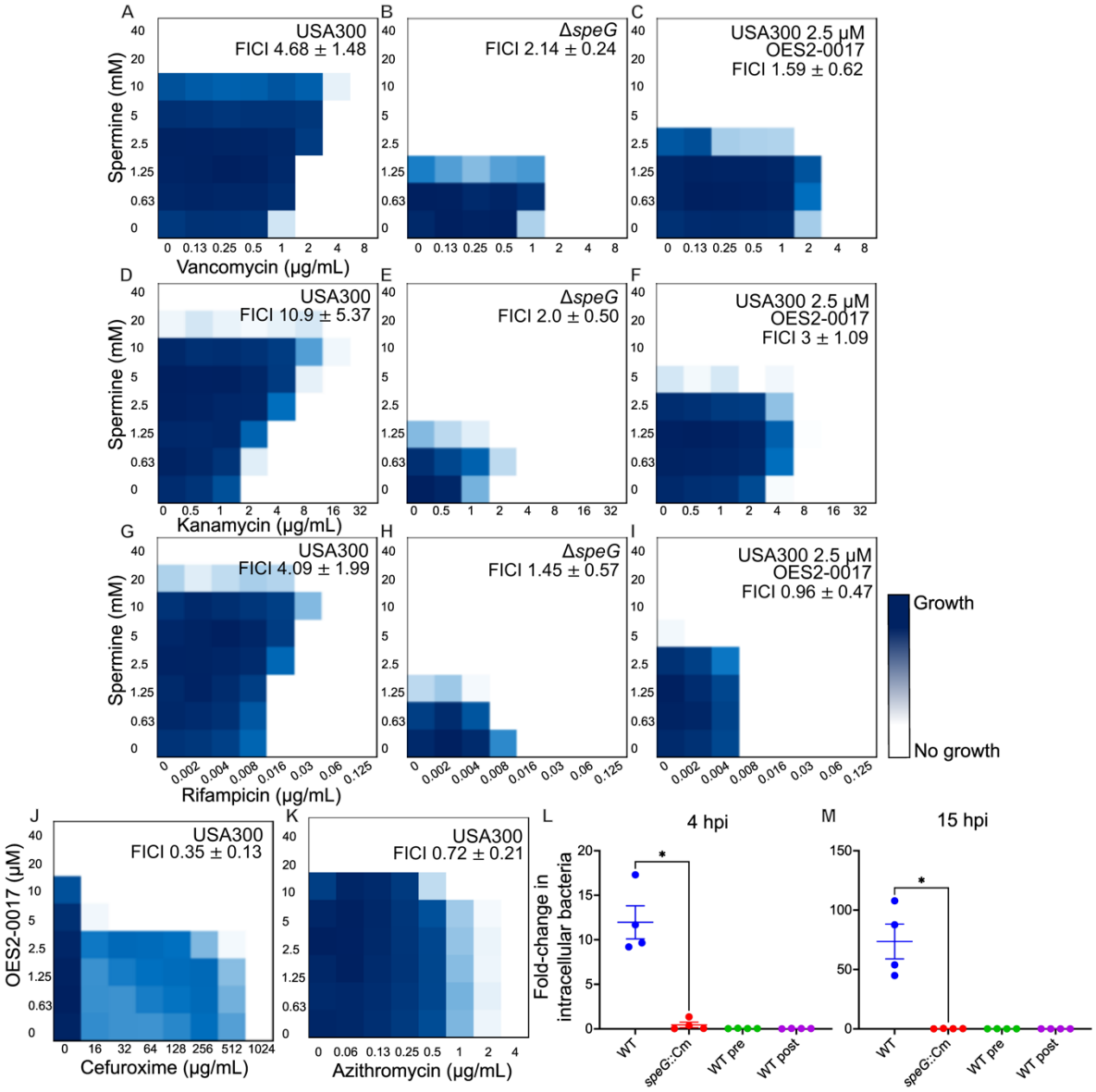

Figure 6. **The potential of OES2-0017 as an antibiotic adjuvant and an antivirulence agent.** Representative checkerboard assays of spermine and vancomycin **(A-C)**, kanamycin **(D-F)**, and rifampicin **(G-I)** against *S. aureus* **A, D, G)** USA300, **B, E, H)** Δ*speG*, and **C, F, I)** USA300 supplemented with a sub-inhibitory concentration of OES2-0017 where OES2-0017 abolishes the protective effect of polyamines from the antibiotics. Representative checkerboard assay of OES2-0017 and cefuroxime **(J)** and azithromycin **(K)** against *S. aureus* USA300, where OES2-0017 potentiates the antibiotic activity. **L** and **M)** murine macrophages treated with OES2-0017 before or after infection with *S.* Typhimurium 14028s or *speG*::Cm and bacterial colony forming units counted at **L)** 4 hours post-infection and **M)** 15 hours post-

704 infection. Data represent 3 independent experiments and statistical analysis was performed by Mann-
705 Whitney test (* signifies $p < 0.05$).

706 **Evaluation of OES2-0017 and OES1-1087 potential eukaryotic activity.** Given the
707 membrane activity of OES2-0017 against *S. aureus* (Figure 4 A and B), we sought to
708 evaluate its potential effects on mammalian cell membranes. To that end, we assessed the
709 hemolytic activity of OES2-0017 against sheep red blood cells. OES2-0017 exhibited
710 hemolytic effects, which are first observed at 160 μM with an increase at 640 μM reaching
711 an absorbance of roughly ½ that of the positive control (Triton X100) (Supplementary Fig.
712 16). The hemolytic effects do occur at a concentration significantly higher than what is
713 necessary to inhibit bacterial growth (8-fold higher than the MIC) or to synergize with
714 spermine through SpeG inhibition (512-fold higher than the lowest point of synergy with
715 spermine). Notably, OES1-1087 did not exhibit hemolytic effects at the concentrations
716 tested (Supplementary Fig. 16). To further evaluate the relative toxicity of OES2-0017 and
717 OES1-0187 toward eukaryotic cells, we also exposed MDCK epithelial cells to the
718 compounds and evaluated their ability to remain adhered to the tissue culture substratum
719 and viable. This analysis revealed that at the *S. aureus* USA300 MIC (1250 μM) OES1-
720 1087 treated cells remain adhered and are refractory to viability dye staining. In contrast,
721 OES2-0017 treated cells detach from the tissue culture substratum at the MIC (20 μM);
722 however, this effect is significantly diminished at ½ the MIC. Moreover, under these same
723 conditions, OES2-0017 treatment does not result in loss of cell viability (Supplementary Fig.
724 17). Altogether, these data indicate that at the concentrations employed in our study
725 significant toxicity towards host cells would not occur.

726 Next, we assessed the activity of OES2-0017 and OES1-1087 against the human
727 spermine/spermidine acetyltransferase, SAT1. SAT1 is a dimer in solution with one
728 monomer seemingly self-acetylating a lysine residue and the other binding polyamines for
729 acetylation (*71*). SpeG and SAT1 are located on two separate branches of the phylogenetic
730 analysis (Supplementary Fig. 13), suggesting a distant relation. A protein alignment by
731 PyMOL 3.0 revealed monomers of the SpeG and SAT1 apoenzymes align well with minor
732 differences in their tertiary structures (PDB ID 5IX3 and 2B5G, respectively; Figure 7 A).
733 However, differences between aligned SpeG and SAT1 are greater when both are bound to
734 substrate (PDB ID 8FV0 and 2BD4, respectively; Figure 7 B). First, we overexpressed and
735 purified SAT1 enzyme and confirmed its acetyltransferase activity *in vitro* with spermine.

SAT1 demonstrated higher substrate specificity (K_M = 73.10 ± 8.328 μM) and high catalytic efficiency (K_{cat}/K_M = 1.28E+05 $M^{-1}s^{-1}$) towards spermine than SpeG (K_M = 1312 ± 348.1 μM and K_{cat}/K_M = 5.58E+03 $M^{-1}s^{-1}$; Supplementary Fig. 18). Our results are in agreement with previous kinetic characterization and the relative activities of both enzymes (*20, 72*). We then tested the ability of OES2-0017 and OES1-1087 to inhibit SAT1. The IC_{50} of OES2-0017 against SAT1 was 26.39 ± 6.411 μM (Figure 7 C), whereas OES1-1087 did not inhibit SAT1 under any of the tested conditions (Supplementary Fig. 18). Although, OES2-0017 can inhibit SAT1 activity, this may not prove detrimental to human cells. Multiple studies have employed the SSAT knockout mice and the non-specific SSAT inhibitor Berenil in *in vivo* mouse models, observing no toxic effects to mice (*73-75*). On the other hand, SAT1 inhibition might have other potential therapeutic uses. Altered polyamine metabolism has been implicated in many human diseases and conditions, including cancer, osteoporosis, and ischemia/reperfusion leading to acute kidney injury (*73, 75-78*) with SAT1 being previously suggested as a promising drug target (*71, 79*).

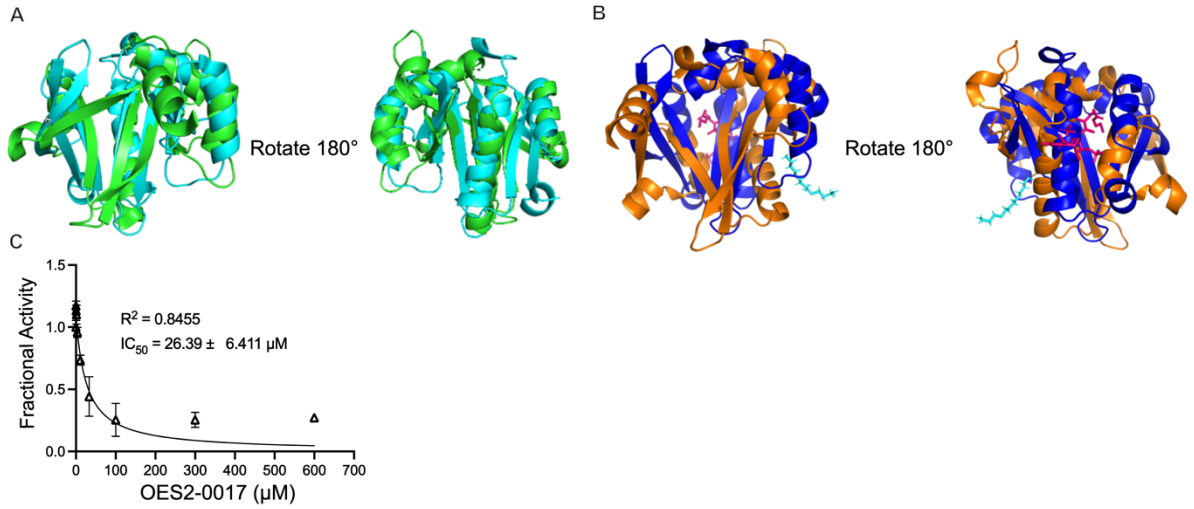

Figure 7. **Effects of OES2-0017 on human SSAT. A)** Structural alignment of human SAT1 (PDB ID 2B5G) represented with green, and *S. aureus* SpeG (PDB ID 5IX3) represented with cyan apoenzymes. **B)** alignment of human SAT1 (PDB ID: 2B4D; orange) co-crystallized with Coenzyme A (magenta) and spermine and *S. aureus* SpeG (PDB ID: 8FV0; blue) co-crystallized with spermine (cyan). Structural alignments were performed using PyMOL 3.0. **C)** Enzymatic inhibition assay performed against human SAT1 with excess AcCoA (0.25 mM) and 75 μM spermine (≈ K_M).

Small-scale structure activity relationship of OES2-0017 suggests the structural components necessary for activity. We performed a small-scale structure

759 activity relationship (SAR) study of OES2-0017 by testing analogs thereof to identify the
760 active moiety of OES2-0017 and detect preferential inhibitory activity against either SpeG or
761 SAT1. The analyses included compounds with varied length of the saturated alkyl chain R_1
762 and one of three R_2 (a proton, an aminoethyl group, or an aminopropyl group) attached on
763 either side of an amine group (Table 1). First, we tested each of the compounds in whole-
764 cell assays in combination with spermine to assess their growth inhibitory and polyamine
765 synergy effects against *S. aureus* USA300. We observed a general reduction in the MIC of
766 the compound as the length of R_1 and R_2 increased (Table 1). Spermine synergy appeared
767 to be dependent on both the length of the alkyl chain and the addition of either the
768 aminoethyl or aminopropyl group. The FICI value decreased (indicating a greater degree of
769 synergy) as the length of the alkyl chain increased; for example, OES2-0047 with R_1 as a
770 proton exhibited no synergy (FICI = 0.88 $\pm$ 0.13) whereas OES2-0052 with R_1 $(CH_2)_5CH_3$
771 showed synergy (FICI = 0.50 $\pm$ 0). The synergistic interaction is further improved when the
772 primary amine is changed to a secondary one with an aminoethyl or aminopropyl; this trend
773 is exemplified in OES2-0046 (R_2 = H; FICI = 0.58 $\pm$ 0.12), OES2-0085 (R_2 = aminoethyl;
774 FICI = 0.56 $\pm$ 0.05), and OES2-0045 (R_2 = aminopropyl; FICI= 0.38 $\pm$ 0).

775 The analogs that synergized with spermine lost the synergy against the Δ*speG*
776 mutant (Table 1), suggesting their synergy is mediated through SpeG inhibition similar to
777 OES2-0017. The analogs that did not exhibit synergy in whole-cell assays are hypothesized
778 to have no SpeG inhibitory activity. Therefore, we tested each compound in enzymatic
779 assays, against both SpeG and SAT1 and estimated K_i values using equation 1 (materials
780 and methods). OES2-0017 remains the most potent inhibitor of SpeG, K_i = 16.25 $\pm$ 3.27 μM
781 with OES2-0052 being the second most potent, K_i = 74.6 $\pm$ 18.28 μM (Table 1 and
782 Supplementary Fig. 19). OES2-0047 and OES2-0046 do not synergize in whole-cell assays
783 and do not inhibit SpeG *in vitro*; thus, they serve as controls to validate the correlation
784 between *in vitro* and whole-cell assays and that our lead compound is targeting and
785 inhibiting SpeG.

786 OES2-0017 inhibited SAT1 with a K_i of 13.03 $\pm$ 4.69 μM, similar to that of SpeG, but
787 the K_i of OES2-0052 is roughly 2-fold higher in SAT1 than SpeG (160.22 $\pm$ 50.45 μM and
788 74.6 $\pm$ 18.28 μM, respectively; Table 1). Similarly, OES2-0077 has almost a two-fold higher
789 K_i against SAT1 than SpeG (743.34 $\pm$ 250.46 and 397.89 $\pm$ 113.0 μM, respectively).

790 Further, two of the tested compounds only inhibited SpeG (OES2-0085 at K_i = 592.08 ±
791 126.15 μM and OES2-0086 at K_i = 559.42 ± 201.51 μM) and not SAT1, in contrast, SAT1
792 activity increased at the highest tested concentrations of these analogs (Supplementary Fig.
793 19). Notably, OES2-0045 which synergized with spermine in whole-cell assays (FICI = 0.38
794 ± 0 μM), suggesting SpeG inhibitory activity, showed no inhibition in the *in vitro* enzymatic
795 assays; however, it inhibited SAT1 (K_i = 227.99 ± 49.73μM; Table 1 and Supplementary
796 Figure 19). These results showing differential activity of some analogs against both
797 enzymes suggest a potential to improve specificity of an inhibitor towards SpeG. Docking
798 the analogs to SpeG or SAT1 revealed that each is expected to bind to the same site as
799 spermine/spermidine, suggesting that all analogs would act in a similar mechanism as
800 OES2-0017 (Supplementary Fig. 20).

801 Given that the compounds also exhibit growth-inhibitory effects, we simultaneously
802 evaluated their hemolytic activity. Hemolytic activity aligned with the MIC data where the
803 concentration required to lyse red blood cells was observed at lower concentrations for
804 compounds with a longer alkyl chain (R_1 = $(CH_2)_3CH_3$ or $(CH_2)_5CH_3$) and with an aminoethyl
805 or aminopropyl group at R_2 (Table 1 and Supplementary Fig. 21). Hemolysis for the SpeG
806 inhibitory compounds OES2-0085 and OES2-0077 occurred at 1280 μM (~2-fold higher
807 than their MICs), while hemolytic activity of OES2-0086, and OES2-0052 was observed at ~
808 4-fold higher than their MICs (640 and 320 μM, respectively; Table 1 and Supplementary
809 Fig. 21). We observed no hemolytic activity of two analogs with high MIC values OES2-
810 0047 and OES2-0046 (Table 1 and Supplementary Fig. 21). The same compounds were
811 also analyzed for their impact on MDCK monolayers which revealed, at their respective
812 MICs against *S. aureus* USA300 and 1 step below (½ MIC), the compounds did not overtly
813 intoxicate eukaryotic cells (Supplementary Fig. 22). Given the promising results of OES2-
814 0052 being more potent against SpeG than SAT1 and lacking observable toxicity against
815 eukaryotic cells, we tested if this compound retains the potential adjuvant activity of OES2-
816 0017. OES2-0052 abolishes the protective effect of spermine towards vancomycin,
817 kanamycin, and rifampicin, and potentiates the activity of cefuroxime (Supplementary Figure
818 23). This analysis provides a foundation for a larger scale targeted lead optimization to
819 improve the potency of SpeG inhibition, while reducing the hemolytic and SAT1 inhibitory
820 activity.

821 Table 1. **Small scale structure activity relationship study of OES2-0017.** SAR study compounds were
822 tested in combination with spermine against *S. aureus* USA300 and Δ*speG*. FICI values are calculated as
823 the mean ± standard deviation of at least three replicates, unless otherwise specified. Inhibitory activity
824 against both SpeG and SAT1 was evaluated in colorimetric enzymatic assays to determine K_i values
825 estimated by the Cheng-Prusoff equation and reported with relative error. Hemolytic activity of each
826 compound was tested against sheep red blood cells.

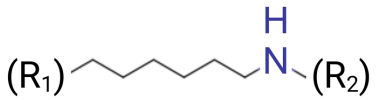

827

Inhibitor	R_1	R_2	MIC (μM)	FICI USA300	FICI Δ*speG*	SpeG K_I (μM)	SAT1 K_I (μM)	Observed hemolysis (μM)
OES2-0047	H	H	2500	0.88 ± 0.13 (n=2)	1.38 ± 0.63 (n=2)	N/A	N/A	None
OES2-0046	CH_2CH_3	H	5000	0.58 ± 0.12	0.92 ± 0.12	N/A	N/A	None
OES2-0085	CH_2CH_3	$(CH_2)_2NH_2$	625	0.56 ± 0.05	1.0 ± 0	592.08 ± 126.15	N/A	1280
OES2-0045	CH_2CH_3	$(CH_2)_3NH_2$	1250	0.38 ± 0	0.67 ± 0.12	N/A	227.99 ± 49.73	1280
OES2-0077	$(CH_2)_3CH_3$	H	625	0.50 ± 0	0.83 ± 0.12	397.89 ±113.0	743.34 ± 250.46	1280
OES2-0086	$(CH_2)_3CH_3$	$(CH_2)_2NH_2$	156.25	0.42 ± 0.12	0.83 ± 0.12	559.42 ± 201.51	N/A	640
OES2-0052	$(CH_2)_5CH_3$	H	62.5	0.50 ± 0	1.25 ± 0.54	74.60 ± 18.28	160.22 ± 50.45	320
OES2-0017	$(CH_2)_5CH_3$	$(CH_2)_3NH_2$	20	0.33 ± 0.06 (n=11)	0.75 ± 0 (n=9)	16.25 ± 3.27	13.03 ± 4.69	160

828

829 **Conclusions**

830 We undertook a chemical screen to identify inhibitors of polyamine detoxification,
831 and uncovered two lead compounds, OES2-0017 and OES1-1087, that show growth
832 inhibition and synergy with spermine. A chemogenomic screen and *in vitro* enzymatic
833 assays revealed that both compounds inhibit the spermine/spermidine acetyltransferase
834 SpeG. The most potent of the two, OES2-0017 with activity at the low micromolar
835 concentration range, inhibited bacterial growth via membrane perturbation. We also
836 observed the growth inhibitory and spermine synergistic effects of OES2-0017 in a broad-

837 spectrum of Gram-positive and Gram-negative bacteria, including *E. faecalis, E. faecium, B.*
838 *cenocepacia, K. pneumoniae,* and *A. baumannii*, and the pathogenic yeast *C. albicans*.
839 Synergy between spermidine and OES2-0017 was not completely lost in a USA300 Δ*speG*
840 mutant, suggesting other underlying polyamine detoxification targets, which prompted us to
841 search for SSATs homologous to *B. subtilis* PaiA and BltD. We found $PaiA_{sa}$, characterized
842 its SSAT activity *in vitro*, and showed that OES2-0017 inhibited its activity. OES2-0017
843 prevented intracellular survival of *S.* Typhimurium in murine macrophages, phenocopying a
844 *speG* deficient mutant. Further, OES2-0017 synergized with cefuroxime and potentiated
845 azithromycin activity against *S. aureus*. This potentiation effect with azithromycin is similar
846 to previous work in *K. pneumoniae* (*30*). OES2-0017 also abolished the ability of *S. aureus*
847 to use exogenous polyamines to resist antibiotic treatment. Finally, we performed a small-
848 scale SAR study and identified compounds with differential activity towards the human
849 SAT1 and *S. aureus* SpeG, including OES2-0086 and OES2-0052. Together, the growth
850 inhibitory effects of the inhibitors identified herein suggest their potential use as stand-alone
851 antimicrobials and their SSAT inhibitory effects, shown to prevent *S.* Typhimurium survival
852 in macrophages, suggest they may serve as antivirulence agents. The synergy with some
853 antibiotics and ability to prevent exogenous polyamine-mediated resistance to other
854 antibiotics in *S. aureus* suggest OES2-0017 may also be used as an antibiotic adjuvant.
855 Polyamine analogs have previously been demonstrated to have antiparasitic,
856 anticancer (*79-81*), and antibacterial properties (*82-84*); however, the previously tested
857 analogs differ in structure from OES2-0017 and the other polyamine analogs tested in this
858 study. Antibacterial polyamines described to date include mono- and bis-acyl polyamines,
859 amine steroidal derivatives (*82*), and diacylpolyamines with aromatic head groups (*83*). One
860 study tested linear polyamine analogs, similar to OES2-0017, and revealed bactericidal and
861 β-lactam potentiating activity; however, the mechanism of growth inhibition and antibiotic
862 potentiation were not discussed (*84*). Notably, several polyamine analogs were shown to
863 inhibit polyamine biosynthesis, transport, and catabolism (*80, 81*). As such, in addition to
864 screening a diverse small molecule library, we also undertook a targeted approach of
865 screening a library of polyamine analogs for activity against polyamine detoxification
866 enzymes. Indeed, this rationale-based approach showed a higher hit rate and higher
867 potencies compared to the unbiased approach although both screens identified SSAT
868 bioactives.

869 Specific bacterial SSAT inhibitors have not been identified previously. Notably,
870 berenil (diminazene aceturate) was shown to inhibit SSAT and has been used *in vivo* in
871 murine models for this purpose (*75*). *In vitro* assays against human SSAT suggested berenil
872 is a potent competitive inhibitor of spermidine with a K_i of 2.0 μM (*85*); however, berenil also
873 inhibits rat S-adenosyl-L-methionine decarboxylase and mouse polyamine oxidase (*85, 86*).
874 Activity against multiple enzymes may explain the toxic effects observed during
875 intramuscular injection of camels with 10 mg/kg berenil (*87*); however no toxic effects were
876 observed in mice dosed at 16 mg/kg weekly for six weeks (*75*) or with a single
877 intraperitoneal or intramuscular dose of 3.5, 10, or 20 mg/kg (*87, 88*). Aside from the SSAT
878 activity, berenil was shown to have other activities, including immunomodulatory(*89*) and
879 cardioprotective(*90*) activities, and is used in veterinary medicine mostly for parasitic
880 infections albeit the exact underlying mode of such activity is not fully elucidated but has
881 been associated with the connection of its aromatic diamidine to the kinetoplast DNA
882 (kDNA) of the trypanosomes(*91*). Our study provides insights that may lead to the
883 development of specific bacterial SSAT inhibitors. Although OES2-0017 caused the
884 detachment of MDCK epithelial cells and hemolytic activity at the MIC and 4X MIC against
885 *S. aureus* USA300, respectively, SpeG-inhibitory activity of the compound was observed as
886 low as 1/32nd the MIC, suggesting a concentration range within which OES2-0017 may
887 remain efficacious while avoiding potential adverse effects. Future studies will further
888 assess the potential toxicity of OES2-0017 and its analogs and their interaction with other
889 polyamine-related enzymes using natural polyamines as substrate.
890 We also identified OES1-1087 (isoproterenol) as a spermine synergist.
891 Isoproterenol is a β1- β2-adrenergic agonist used in the treatment of heart block, heart
892 failure, and cardiac arrest (*92*). Its identification in our chemical screen serves as an
893 example of potential drug repurposing for the treatment of bacterial infections. Time and
894 money spent on drug development are drastically reduced by repurposing as
895 pharmacodynamic, pharmacokinetic, and toxicity profiles of the drugs are already known
896 (*93*). Our results indicate that isoproterenol also inhibits SpeG, albeit with much lower
897 potency than OES2-0017, and exhibits growth inhibitory activity. Importantly, it did not show
898 detectable activity against the human SAT1 and no hemolytic activity or adverse effects on
899 MDCK epithelial cell adherence or viability.

900 The cellular concentrations of polyamines in mammalian cells vary across tissues
901 and physiological conditions; however, the total polyamine content is generally assessed to
902 be in the mM range (*16*). Polyamines are known to bind to macromolecules, such as DNA,
903 RNA, phospholipids, and ATP, so levels of free intracellular polyamines are not definitive
904 (*16*). In polyamine-producing bacteria, the contents of intracellular polyamines have been
905 reported as high as 30 mM (*16*). Importantly, polyamine concentrations in the host further
906 increase ~2-fold in response to infection (*14*). As such, bacteria are likely to encounter
907 polyamines during infection or in their surrounding environment at concentrations similar or
908 higher than those tested in this study. Further, the detrimental effects of *speG* or alternative
909 SSAT mutations on bacterial virulence (*14, 24, 25*) suggest that the levels of polyamines
910 within the host are comparable to those used *in vitro* at which polyamine susceptibility and
911 synergy with the inhibitors were observed in this study. Therefore, given that OES2-0017
912 inhibits *speG,* it will likely reduce the ability of bacteria to withstand host polyamines
913 produced at the site of infection, suggesting it may allow these host compounds to help
914 clear infection serving as antivirulence agent.
915 *In vitro* enzymatic assays suggest that OES2-0017 is relatively equipotent against
916 both SpeG and SAT1 suggesting potential activity against the human enzyme *in vivo*. SAT1
917 inhibitors have other potential therapeutic uses including disrupting tumor growth, protection
918 from kidney injury following ischemia-reperfusion injury, and preventing osteoporosis (*71,*
919 *73, 75, 79*). Notably, there were two analogs of OES2-0017, OES2-0085 and OES2-0086,
920 that showed inhibitory activity against SpeG but not SAT1 and another two, OES2-0077 and
921 OES2-0052, which were more potent inhibitors of SpeG than SAT1. Although these analogs
922 have lower inhibitory activity than OES2-0017, they and other analogs from our analysis can
923 guide future SAR studies to optimize the inhibition of SpeG while limiting activity against
924 SAT1.

925 *S. aureus* was not previously known to have an SSAT except for strains that
926 acquired SpeG, such as USA300. Notably, the USA300 Δ*speG* and other *S. aureus* strains
927 that do not harbor *speG* (e.g., COL and NCTC8325) are only 4-fold and 8-fold more
928 susceptible to spermidine and spermine, respectively, compared to wild-type USA300,
929 suggesting a potential for another detoxification mechanism. Here, we identified $PaiA_{Sa}$, a
930 homolog of *B. subtilis* spermine/spermidine acetyltransferase PaiA, in *S. aureus,* providing
931 its first experimental characterization as an additional SSAT in *S. aureus*. SpeG appears to

932 be more dominant with a greater shift in polyamine susceptibility observed in a Δ*speG*
933 mutant than *paiA*$_{Sa}$::Tn; the contribution of PaiA$_{Sa}$ to polyamine resistance in whole cells
934 requires assessment in a *speG paiA*$_{Sa}$ double mutant in USA300 or a single *paiA*$_{Sa}$ mutant
935 in a *speG*$^{-}$ *S. aureus* strain. We further showed that OES2-0017 can inhibit PaiA$_{Sa}$ *in vitro.*
936 This work provides insights into understudied aspects of chemically mediated host-
937 pathogen interactions. We discovered two novel inhibitors of spermine/spermidine *N*-
938 acetyltransferase. The discovered inhibitors have potential application as stand-alone
939 antimicrobials, antivirulence agents, or antibiotic adjuvants. This work provides antimicrobial
940 compounds with a novel mechanism for the fight against multidrug-resistant priority
941 pathogens.
942
943 **Acknowledgements**
944 This work was supported by Natural Sciences and Engineering Research Council of
945 Canada discovery grant (RGPIN-2022-04239 and DGECR-2022- 00206), a Saskatchewan
946 Health Research Foundation establishment grant (6115), and start-up funds from the Faculty
947 of Science at the University of Regina to OME. OME holds a Canada Research Chair in
948 Chemogenomics and Antimicrobial Research (CRC-2019- 00115). PBM and JW were
949 supported by a Canadian Institutes of Health Research Canada Graduate Scholarship—
950 Master's (CGS-M) award. PBM was also supported by the Verna Martin Memorial
951 Scholarship. WE holds a Canada Research Chair in Microbiome Research (CRC-00249). WE
952 is funded by Crohn's & Colitis Canada, Natural Sciences and Engineering Research Council
953 of Canada, Major Innovation Fund, Antimicrobial Resistance - One Health Consortium, and
954 Striving for Pandemic Preparedness - The Alberta Research Consortium (SPP-ARC). Work
955 in the DEH laboratory was funded by an operating grant (PJT-183848) from the Canadian
956 Institutes of Health Research.
957

References

1. C. J. Murray *et al.*, Global burden of bacterial antimicrobial resistance in 2019: a systematic analysis. *Lancet* **399**, 629-655 (2022).
2. WHO, *Prioritization of pathogens to guide discovery, research and development of new antibiotics for drug-resistant bacterial infections, including tuberculosis*. (World Health Organization, Geneva, 2017).
3. T. A. Taylor, C. G. Unakal, in *StatPearls*. (Treasure Island (FL), 2023).
4. K. A. Nichol *et al.*, Characterization of MRSA in Canada from 2007 to 2016. *J Antimicrob Chemother* **74**, iv55-iv63 (2019).
5. D. J. Diekema *et al.*, Continued emergence of USA300 methicillin-resistant Staphylococcus aureus in the United States: results from a nationwide surveillance study. *Infect Control Hosp Epidemiol* **35**, 285-292 (2014).
6. P. Beyer, S. Paulin, The Antibacterial Research and Development Pipeline Needs Urgent Solutions. *ACS Infect Dis* **6**, 1289-1291 (2020).
7. M. Miethke *et al.*, Towards the sustainable discovery and development of new antibiotics. *Nat Rev Chem* **5**, 726-749 (2021).
8. CLSI, *Methods for Dilution Antimicrobial Susceptibility Tests for Bacteria that Grow Aerobically Approved Standard—Tenth Edition M07-A10*. (2012).
9. O. M. El-Halfawy, M. A. Valvano, Non-genetic mechanisms communicating antibiotic resistance: rethinking strategies for antimicrobial drug design. *Expert Opin Drug Discov* **7**, 923-933 (2012).
10. P. B. Moulding, O. M. El-Halfawy, Chemical-mediated virulence: the effects of host chemicals on microbial virulence and potential new antivirulence strategies. *Canadian journal of microbiology*, (2024).
11. C. W. Tabor, H. Tabor, Polyamines. *Annu Rev Biochem* **53**, 749-790 (1984).
12. X. Yao, C. D. Lu, Functional characterization of the potRABCD operon for spermine and spermidine uptake and regulation in Staphylococcus aureus. *Curr Microbiol* **69**, 75-81 (2014).
13. A. F. Gazdar, H. B. Stull, L. J. Kilton, U. Bachrach, Increased ornithine decarboxylase activity in murine sarcoma virus infected cells. *Nature* **262**, 696-698 (1976).
14. L. R. Thurlow *et al.*, Functional modularity of the arginine catabolic mobile element contributes to the success of USA300 methicillin-resistant *Staphylococcus aureus*. *Cell Host Microbe* **13**, 100-107 (2013).
15. S. Watanabe, K. Kusama-Eguchi, H. Kobayashi, K. Igarashi, Estimation of polyamine binding to macromolecules and ATP in bovine lymphocytes and rat liver. *J Biol Chem* **266**, 20803-20809 (1991).
16. K. Igarashi, K. Kashiwagi, Modulation of cellular function by polyamines. *Int J Biochem Cell Biol* **42**, 39-51 (2010).
17. C. Moinard, L. Cynober, J. P. de Bandt, Polyamines: metabolism and implications in human diseases. *Clin Nutr* **24**, 184-197 (2005).
18. M. Zhang, H. Wang, K. J. Tracey, Regulation of macrophage activation and inflammation by spermine: a new chapter in an old story. *Crit Care Med* **28**, N60-66 (2000).
19. G. S. Joshi, J. S. Spontak, D. G. Klapper, A. R. Richardson, Arginine catabolic mobile element encoded *speG* abrogates the unique hypersensitivity of *Staphylococcus aureus* to exogenous polyamines. *Mol Microbiol* **82**, 9-20 (2011).
20. B. Li *et al.*, Polyamine-independent growth and biofilm formation, and functional spermidine/spermine N-acetyltransferases in *Staphylococcus aureus* and *Enterococcus faecalis*. *Mol Microbiol* **111**, 159-175 (2019).
21. J. Seravalli, F. Portugal, , Putrescine Detected in Strains of Staphylococcus aureus. *Pathogens* **12**, 881 (2023).

1008 22. B. A. Diep *et al.*, The arginine catabolic mobile element and staphylococcal
1009 chromosomal cassette mec linkage: convergence of virulence and resistance in the
1010 USA300 clone of methicillin-resistant Staphylococcus aureus. *J Infect Dis* **197**, 1523-
1011 1530 (2008).
1012 23. P. J. Planet *et al.*, Emergence of the epidemic methicillin-resistant *Staphylococcus*
1013 *aureus* strain USA300 coincides with horizontal transfer of the arginine catabolic mobile
1014 element and *speG*-mediated adaptations for survival on skin. *MBio* **4**, e00889-00813
1015 (2013).
1016 24. S. B. Fang *et al.*, *speG* Is Required for Intracellular Replication of *Salmonella* in Various
1017 Human Cells and Affects Its Polyamine Metabolism and Global Transcriptomes. *Front*
1018 *Microbiol* **8**, (2017).
1019 25. C. Martini *et al.*, The polyamine N-acetyltransferase-like enzyme PmvE plays a role in
1020 the virulence of *Enterococcus faecalis*. *Infect Immun* **83**, 364-371 (2015).
1021 26. X. Yao, C. D. Lu, A PBP 2 mutant devoid of the transpeptidase domain abolishes
1022 spermine-beta-lactam synergy in *Staphylococcus aureus* Mu50. *Antimicrob Agents*
1023 *Chemother* **56**, 83-91 (2012).
1024 27. D. H. Kwon, C. D. Lu, Polyamines induce resistance to cationic peptide, aminoglycoside,
1025 and quinolone antibiotics in *Pseudomonas aeruginosa* PAO1. *Antimicrob Agents*
1026 *Chemother* **50**, 1615-1622 (2006).
1027 28. D. H. Kwon, C. D. Lu, Polyamine effects on antibiotic susceptibility in bacteria.
1028 *Antimicrob Agents Chemother* **51**, 2070-2077 (2007).
1029 29. J. Li, R. Beuerman, C. S. Verma, Mechanism of polyamine induced colistin resistance
1030 through electrostatic networks on bacterial outer membranes. *Biochim Biophys Acta*
1031 *Biomembr* **1862**, 183297 (2020).
1032 30. J. M. E. Adams, P. B. Moulding, O. M. El-Halfawy, Polyamine-Mediated Sensitization of
1033 *Klebsiella pneumoniae* to Macrolides through a Dual Mode of Action. *ACS Infect Dis* **10**,
1034 2183-2195 (2024).
1035 31. M. W. McGinnis *et al.*, Spermidine regulates Vibrio cholerae biofilm formation via
1036 transport and signaling pathways. *FEMS Microbiol Lett* **299**, 166-174 (2009).
1037 32. Z. Liu, S. S. Hossain, Z. Morales Moreira, C. H. Haney, Putrescine and Its Metabolic
1038 Precursor Arginine Promote Biofilm and c-di-GMP Synthesis in *Pseudomonas*
1039 *aeruginosa*. *J Bacteriol* **204**, e0029721 (2022).
1040 33. C. N. Patel *et al.*, Polyamines are essential for the formation of plague biofilm. *J*
1041 *Bacteriol* **188**, 2355-2363 (2006).
1042 34. G. K. Nasrallah *et al.*, Legionella pneumophila requires polyamines for optimal
1043 intracellular growth. *J Bacteriol* **193**, 4346-4360 (2011).
1044 35. P. Shah, B. Nanduri, E. Swiatlo, Y. Ma, K. Pendarvis, Polyamine biosynthesis and
1045 transport mechanisms are crucial for fitness and pathogenesis of Streptococcus
1046 pneumoniae. *Microbiology (Reading)* **157**, 504-515 (2011).
1047 36. L. Johnson, H. Mulcahy, U. Kanevets, Y. Shi, S. Lewenza, Surface-localized spermidine
1048 protects the Pseudomonas aeruginosa outer membrane from antibiotic treatment and
1049 oxidative stress. *J Bacteriol* **194**, 813-826 (2012).
1050 37. S. W. Dickey, G. Y. C. Cheung, M. Otto, Different drugs for bad bugs: antivirulence
1051 strategies in the age of antibiotic resistance. *Nat Rev Drug Discov* **16**, 457-471 (2017).
1052 38. G. Dhanda, Y. Acharya, J. Haldar, Antibiotic Adjuvants: A Versatile Approach to Combat
1053 Antibiotic Resistance. *ACS Omega* **8**, 10757-10783 (2023).
1054 39. P. D. Fey *et al.*, A genetic resource for rapid and comprehensive phenotype screening of
1055 nonessential *Staphylococcus aureus* genes. *MBio* **4**, e00537-00512 (2013).
1056 40. J. M. Peters *et al.*, A comprehensive, CRISPR-based functional analysis of essential
1057 genes in bacteria. *Cell* **165**, 1493-1506 (2016).

41. J. L. Bose, P. D. Fey, K. W. Bayles, Genetic tools to enhance the study of gene function and regulation in Staphylococcus aureus. *Appl Environ Microbiol* **79**, 2218-2224 (2013).
42. M. R. Grosser, A. R. Richardson, Method for Preparation and Electroporation of *S. aureus* and *S. epidermidis*. *Methods Mol Biol* **1373**, 51-57 (2016).
43. M. A. Farha, C. P. Verschoor, D. Bowdish, E. D. Brown, Collapsing the proton motive force to identify synergistic combinations against *Staphylococcus aureus*. *Chem Biol* **20**, 1168-1178 (2013).
44. W. T. Barker, C. E. Chandler, R. J. Melander, R. K. Ernst, C. Melander, Tryptamine derivatives disarm colistin resistance in polymyxin-resistant gram-negative bacteria. *Bioorg Med Chem* **27**, 1776-1788 (2019).
45. H. J. Lin, Y. C. Lien, C. H. Hsu, A high-throughput colorimetric assay to characterize the enzyme kinetic and cellular activity of spermidine/spermine N1-acetyltransferase 1. *Anal Biochem* **407**, 226-232 (2010).
46. Y. Cheng, W. H. Prusoff, Relationship between the inhibition constant (K1) and the concentration of inhibitor which causes 50 per cent inhibition (I50) of an enzymatic reaction. *Biochem Pharmacol* **22**, 3099-3108 (1973).
47. O. M. El-Halfawy, M. A. Valvano, Chemical communication of antibiotic resistance by a highly resistant subpopulation of bacterial cells. *PLOS One* **8**, e68874 (2013).
48. A. Kallio, P. P. McCann, Difluoromethylornithine irreversibly inactivates ornithine decarboxylase of Pseudomonas aeruginosa, but does not inhibit the enzymes of Escherichia coli. *Biochem J* **200**, 69-75 (1981).
49. T. Mattila, T. Honkanen-Buzalski, H. Poso, Reversible inhibition of bacterial growth after specific inhibition of spermidine synthase by dicyclohexylamine. *Biochem J* **223**, 823-830 (1984).
50. H. Maki, N. McCallum, M. Bischoff, A. Wada, B. Berger-Bachi, tcaA inactivation increases glycopeptide resistance in Staphylococcus aureus. *Antimicrob Agents Chemother* **48**, 1953-1959 (2004).
51. M. Tsai *et al.*, Staphylococcus aureus requires cardiolipin for survival under conditions of high salinity. *BMC Microbiol* **11**, 13 (2011).
52. F. C. Beasley, J. Cheung, D. E. Heinrichs, Mutation of L-2,3-diaminopropionic acid synthase genes blocks staphyloferrin B synthesis in *Staphylococcus aureus*. *BMC Microbiol* **11**, 199 (2011).
53. S. Tsimbalyuk *et al.*, Structural and Kinetic Characterization of the SpeG Spermidine/Spermine N-acetyltransferase from Methicillin-Resistant Staphylococcus aureus USA300. *Cells* **12**, (2023).
54. J. Zhu, I. Dhimitruka, D. Pei, 5-(2-Aminoethyl)dithio-2-nitrobenzoate as a more base-stable alternative to Ellman's reagent. *Org Lett* **6**, 3809-3812 (2004).
55. E. V. Filippova *et al.*, A novel polyamine allosteric site of SpeG from Vibrio cholerae is revealed by its dodecameric structure. *J Mol Biol* **427**, 1316-1334 (2015).
56. S. Tsimbalyuk, A. Shornikov, V. Thi Bich Le, M. L. Kuhn, J. K. Forwood, SpeG polyamine acetyltransferase enzyme from Bacillus thuringiensis forms a dodecameric structure and exhibits high catalytic efficiency. *J Struct Biol* **210**, 107506 (2020).
57. V. T. B. Le *et al.*, The Vibrio cholerae SpeG Spermidine/Spermine N-Acetyltransferase Allosteric Loop and beta6-beta7 Structural Elements Are Critical for Kinetic Activity. *Front Mol Biosci* **8**, 645768 (2021).
58. E. V. Filippova *et al.*, Substrate-Induced Allosteric Change in the Quaternary Structure of the Spermidine N-Acetyltransferase SpeG. *J Mol Biol* **427**, 3538-3553 (2015).
59. D. P. Woolridge, J. D. Martinez, D. E. Stringer, E. W. Gerner, Characterization of a novel spermidine/spermine acetyltransferase, BltD, from Bacillus subtilis. *Biochem J* **340 (Pt 3)**, 753-758 (1999).

1108 60. F. Forouhar *et al.*, Structural and functional evidence for Bacillus subtilis PaiA as a novel
1109 N1-spermidine/spermine acetyltransferase. *J Biol Chem* **280**, 40328-40336 (2005).
1110 61. K. Yasuda, C. Ohmizo, T. Katsu, Mode of action of novel polyamines increasing the
1111 permeability of bacterial outer membrane. *Int J Antimicrob Agents* **24**, 67-71 (2004).
1112 62. J. Armalyte *et al.*, A polyamine acetyltransferase regulates the motility and biofilm
1113 formation of Acinetobacter baumannii. *Nat Commun* **14**, 3531 (2023).
1114 63. I. Matsui, M. Kamei, S. Otani, S. Morisawa, A. E. Pegg, Occurrence and induction of
1115 spermidine-N1-acetyltransferase in Escherichia coli. *Biochem Biophys Res Commun*
1116 **106**, 1155-1160 (1982).
1117 64. L. I. Hu *et al.*, The spermidine acetyltransferase SpeG regulates transcription of the
1118 small RNA rprA. *PLoS One* **13**, e0207563 (2018).
1119 65. *WHO Bacterial Priority Pathogens List, 2024: bacterial pathogens of public health*
1120 *importance to guide research, development and strategies to prevent and control*
1121 *antimicrobial resistance*. (World Health Organization, Geneva, 2024).
1122 66. T. E. Dever, I. P. Ivanov, Roles of polyamines in translation. *J Biol Chem* **293**, 18719-
1123 18729 (2018).
1124 67. K. Igarashi, K. Kashiwagi, Polyamines: mysterious modulators of cellular functions.
1125 *Biochem Biophys Res Commun* **271**, 559-564 (2000).
1126 68. W. T. Liu *et al.*, Emerging resistance mechanisms for 4 types of common anti-MRSA
1127 antibiotics in Staphylococcus aureus: A comprehensive review. *Microb Pathog* **156**,
1128 104915 (2021).
1129 69. H. Ma *et al.*, Adjunctive rifampin for the treatment of Staphylococcus aureus bacteremia
1130 with deep infections: A meta-analysis. *PLoS One* **15**, e0230383 (2020).
1131 70. E. J. Choo, H. F. Chambers, Treatment of Methicillin-Resistant Staphylococcus aureus
1132 Bacteremia. *Infect Chemother* **48**, 267-273 (2016).
1133 71. M. C. Bewley *et al.*, Structures of wild-type and mutant human spermidine/spermine N1-
1134 acetyltransferase, a potential therapeutic drug target. *Proc Natl Acad Sci U S A* **103**,
1135 2063-2068 (2006).
1136 72. S. S. Hegde, J. Chandler, M. W. Vetting, M. Yu, J. S. Blanchard, Mechanistic and
1137 structural analysis of human spermidine/spermine N1-acetyltransferase. *Biochemistry*
1138 **46**, 7187-7195 (2007).
1139 73. K. Zahedi *et al.*, Spermidine/spermine-N1-acetyltransferase ablation protects against
1140 liver and kidney ischemia-reperfusion injury in mice. *Am J Physiol Gastrointest Liver*
1141 *Physiol* **296**, G899-909 (2009).
1142 74. J. Xu *et al.*, Inhibition of SAT1 alleviates chondrocyte inflammation and ferroptosis by
1143 repressing ALOX15 expression and activating the Nrf2 pathway. *Bone Joint Res* **13**,
1144 110-123 (2024).
1145 75. Z. Jin, H. Xu, X. Sun, B. Yan, L. Wang, Targeting SAT1 prevents osteoporosis through
1146 promoting osteoclast apoptosis. *Biomed Pharmacother* **175**, 116732 (2024).
1147 76. K. Zahedi, S. Barone, M. Soleimani, Polyamine Catabolism in Acute Kidney Injury. *Int J*
1148 *Mol Sci* **20**, (2019).
1149 77. D. H. Russell, Increased polyamine concentrations in the urine of human cancer
1150 patients. *Nat New Biol* **233**, 144-145 (1971).
1151 78. A. W. Maksymiuk *et al.*, Spermidine/spermine N1-acetyltransferase-1 as a diagnostic
1152 biomarker in human cancer. *Future Sci OA* **4**, FSO345 (2018).
1153 79. H. M. Wallace, A. V. Fraser, Inhibitors of polyamine metabolism: review article. *Amino*
1154 *Acids* **26**, 353-365 (2004).
1155 80. O. S. Egorov *et al.*, Structure and biological action of analogs and derivatives of biogenic
1156 polyamines. *Fine Chemical Technologies* **16**, 287-306 (2021).

1157 81. T. Boncher, X. Bi, S. Varghese, R. A. Casero, Jr., P. M. Woster, Polyamine-based
1158 analogues as biochemical probes and potential therapeutics. *Biochem Soc Trans* **35**,
1159 356-363 (2007).
1160 82. M. Blanchet, D. Borselli, J. M. Brunel, Polyamine derivatives: a revival of an old
1161 neglected scaffold to fight resistant Gram-negative bacteria? *Future Med Chem* **8**, 963-
1162 973 (2016).
1163 83. D. Chen *et al.*, alpha,omega-Diacyl-Substituted Analogues of Natural and Unnatural
1164 Polyamines: Identification of Potent Bactericides That Selectively Target Bacterial
1165 Membranes. *Int J Mol Sci* **24**, (2023).
1166 84. E. J. A. Douglas *et al.*, Antibacterial activity of novel linear polyamines against
1167 Staphylococcus aureus. *Front Microbiol* **13**, 948343 (2022).
1168 85. P. R. Libby, C. W. Porter, Inhibition of enzymes of polyamine back-conversion by
1169 pentamidine and berenil. *Biochem Pharmacol* **44**, 830-832 (1992).
1170 86. E. Karvonen, L. Kauppinen, T. Partanen, H. Poso, Irreversible inhibition of putrescine-
1171 stimulated S-adenosyl-L-methionine decarboxylase by berenil and pentamidine.
1172 *Biochem J* **231**, 165-169 (1985).
1173 87. A. M. Homeida, E. A. El Amin, S. E. Adam, M. M. Mahmoud, Toxicity of diminazene
1174 aceturate (Berenil) to camels. *J Comp Pathol* **91**, 355-360 (1981).
1175 88. E. A. Elamin, A. M. Homeida, S. E. Adam, M. M. Mahmoud, The efficacy of berenil
1176 (diminazene aceturate) against Trypanosoma evansi infection in mice. *J Vet Pharmacol*
1177 *Ther* **5**, 259-265 (1982).
1178 89. P. Passaglia *et al.*, Diminazene aceturate attenuates systemic inflammation via
1179 microbiota gut-5-HT brain-spleen sympathetic axis in male mice. *Brain Behav Immun*
1180 **119**, 105-119 (2024).
1181 90. D. C. O. Coutinho *et al.*, Diminazene Aceturate, an angiotensin converting enzyme 2
1182 (ACE2) activator, promotes cardioprotection in ischemia/reperfusion-induced cardiac
1183 injury. *Peptides* **151**, 170746 (2022).
1184 91. G. L. da Silva Oliveira, R. M. de Freitas, Diminazene aceturate--An antiparasitic drug of
1185 antiquity: Advances in pharmacology & therapeutics. *Pharmacol Res* **102**, 138-157
1186 (2015).
1187 92. Isoproterenol. (Medscape - https://reference.medscape.com/drug/isuprel-isoproterenol-
1188 342438#91, 2024).
1189 93. M. A. Farha, E. D. Brown, Drug repurposing for antimicrobial discovery. *Nat Microbiol* **4**,
1190 565-577 (2019).

1191

1192

1193

1194